AD-A011 807

EFFECTS OF CHARGE SHAPE AND COMPOSITIO:: ON BLAST ENVIRONMENT

J. E. Tancreto

Civil Engineering Laboratory (Navy)

Prepared for:

Picatinny Arsenal

May 1975

DISTRIBUTED BY:

NTIS

National Technical Information Service
U. S. DEPARTMENT OF COMMERCE

1 96092

ADA011807

Technical Note N-1390

EFFECTS OF CHARGE SHAPE AND COMPOSITION ON BLAST ENVIRONMENT

by

J. E. Tancreto

May 1975

Sponsored by

PICATINNY ARSENAL

CIVIL ENGINEERING LABORATORY
Naval Construction Battalion Center
Port Hueneme, CA 93043

20. Continued

but surface hardness and slight charge elevation effects were also investigated.

Peak-pressure and peak-scaled unit impulse equivalencies (by weight of TNT hemispherical surface bursts) are calculated for composition B spheres and cylinders and for the RDX slurry charges. Test results indicate that the blast environment from composition B depends more on the shape of the charge than on its chemical difference from the TNT standard. The composition B equivalencies determined in this study might be more properly labeled as shape factors which could be applied to any high explosive.

Civil Engineering Laboratory
EFFECTS OF CHARGE SHAPE AND COMPOSITION ON BLAST ENVIRONMENT (Final), by J. E. Tancreto
TN-1390 56 p. illus May 1975 Unclassified

1. Blast environment - charge shape effects I. 51-027

Blast pressures were obtained from surface bursts of hemispherical, spherical, and cylindrical composition B explosive and from encased RDX slurry charges. Charge weights varied from 0.50 to 3.7 pounds. Pressure measurements, taken between 2 and 50 feet from the charge, varied from less than 1 psi to over 1,000 psi.

The pressure-time records were evaluated for peak pressure, impulse, and positive-phase duration. The effects of charge shape and composition were of primary importance, but surface hardness and slight charge elevation effects were also investigated.

Peak-pressure and peak-scaled unit impulse equivalencies (by weight of TNT hemispherical surface bursts) are calculated for composition B spheres and cylinders and for the RDX slurry charges. Test results indicate that the blast environment from composition B depends more on the shape of the charge than on its chemical difference from the TNT standard. The composition B equivalencies determined in this study might be more properly labeled as shape factors which could be applied to any high explosive.

Unclassified

SECURITY CLASSIFICATION OF THIS PAGE (When Data Entered)

REPORT DOCUMENTATION PAGE		READ INSTRUCTIONS BEFORE COMPLETING FORM
1. REPORT NUMBER TN-1390	2. GOVT ACCESSION NO. DN244065	3. RECIPIENT'S CATALOG NUMBER
4. TITLE (and Subtitle) EFFECTS OF CHARGE SHAPE AND COMPOSITION ON BLAST ENVIRONMENT		5. TYPE OF REPORT & PERIOD COVERED Final; Mar 1972–Sep 1974 6. PERFORMING ORG. REPORT NUMBER
7. AUTHOR(s) J. E. Tancreto		8. CONTRACT OR GRANT NUMBER(s)
9. PERFORMING ORGANIZATION NAME AND ADDRESS CIVIL ENGINEERING LABORATORY Naval Construction Battalion Center Port Hueneme, California 93043		10. PROGRAM ELEMENT, PROJECT, TASK AREA & WORK UNIT NUMBERS Army MIPR; 51-027
11. CONTROLLING OFFICE NAME AND ADDRESS Picatinny Arsenal Dover, New Jersey 07801		12. REPORT DATE May 1975 13. NUMBER OF PAGES 62
14. MONITORING AGENCY NAME & ADDRESS (if different from Controlling Office)		15. SECURITY CLASS. (of this report) Unclassified 15a. DECLASSIFICATION DOWNGRADING SCHEDULE

16. DISTRIBUTION STATEMENT (of this Report)

Approved for public release; distribution unlimited.

17. DISTRIBUTION STATEMENT (of the abstract entered in Block 20, if different from Report)

18. SUPPLEMENTARY NOTES

19. KEY WORDS (Continue on reverse side if necessary and identify by block number)

(U) Explosive storage; (U) explosive effects; (U) cubicles; (U) magazine; (U) TNT equivalency.

20. ABSTRACT (Continue on reverse side if necessary and identify by block number)

Blast pressures were obtained from surface bursts of hemispherical, spherical, and cylindrical composition B explosive and from encased RDX slurry charges. Charge weights varied from 0.50 to 3.7 pounds. Pressure measurements, taken between 2 and 50 feet from the charge, varied from less than 1 psi to over 1,000 psi.

The pressure-time records were evaluated for peak pressure, impulse, and positive-phase duration. The effects of charge shape and composition were of primary importance,

continued

DD FORM 1 JAN 73 1473 EDITION OF 1 NOV 65 IS OBSOLETE

Unclassified

SECURITY CLASSIFICATION OF THIS PAGE (When Data Entered)

CONTENTS

LIST OF ILLUSTRATIONS

		Page

LIST OF TABLES

INTRODUCTION

The U. S. Army Armament Command (ARMCOM) is modernizing ammunition facilities, including equipment and protective structures, used in manufacturing, processing, and storage of conventional munitions. Consistent with new safety regulations, those structures which serve to prevent explosive propagation, damage to material, or injury to personnel are being designed to comply with criteria and methods set forth in the TM5-1300 Manual, ''Structures to Resist the Effects of Accidental Explosions'' [1]. The manual contains methods and criteria for determining the blast environment and its effect on personnel, structure, and adjacent explosives.

A scale-model cubicle test program to supplement material in TM5-1300 is being sponsored by Picatinny Arsenal (Manufacturing Technology Directorate) and conducted by the Navy's Civil Engineering Laboratory (CEL), Port Hueneme, CA. The cubicle test program was designed to establish the blast environment in and around fully and partially vented cubicles. A CEL report [2] presents the cubicle test program results and gives methods and criteria for predicting the blast environment for practical variations in critical parameters, including the size, shape, and vent area of the cubicle, and the charge weight inside the cubicle. The influence of cover frangibility is presently being studied at CEL and will be the subject of another report.

Because of the large number of tests and the small size of the test charges, composition B cylinders were chosen as the explosive for the cubicle test program. Composition B is easier to detonate in small amounts [3], and cylinders are less expensive than spheres. It is, therefore, necessary to relate the output of a composition B cylinder to that of an established standard such as a TNT hemispherical surface burst given in TM5-1300. The effects of charge shape and composition can then be accounted for when the results of the scale-model cubicle tests are incorporated into TM5-1300.

RDX slurry tanks are used in ammunition production facilities. The shock wave parameters from an accidental explosion of such a tank is important in the design of new facilities. The test site used for determining the composition B equivalency was also used to determine the output of RDX slurry.

OBJECTIVE

The primary test objectives were to measure the pressure-time-distance relationships for surface bursts of cylindrical composition B and for encased RDX slurry high explosives and to study the effects

of charge shape. Included in the study of charge shape effects was a direct comparison of pressure-time data from the detonation of spheres and cylinders in a cubicle.

Secondary objectives included the study of the effects of surface hardness and small heights of bursts on air-blast parameters. The effects of using composition B cylinders in a future scale model cubicle test program were also evaluated.

EXPERIMENTAL PROGRAM

Test Planning

The original test plan specified a direct comparison of air-blast parameters from composition B cylinders and RDX slurry containers to those from TNT spheres. All charges were elevated (the cylinders and spheres were elevated 3 radii from ground level to the center of gravity; the center of gravity of the precipitated RDX disc in the slurry container was elevated 3 radii of a sphere of the same weight). Good data was obtained from the composition B and RDX slurry tests. However, poor detonation of the center-initiated cast TNT spheres prevented use of the TNT data for comparison. Similar problems with TNT spheres were reported by Fisher and Pitmann [3].

The test program was then expanded to include surface bursts of composition B hemispheres, spheres, and cylinders. The spherical and hemispherical data could be compared with known TNT surface burst results for determination of TNT equivalency of composition B and to check out the pressure measurement system. Table 1 summarizes the scope of the test program.

The hemispherical composition B charges were detonated on sand and on a steel plate to determine which condition produced the most consistent results for surface bursts. The test results indicated that the steel plate should be used for subsequent testing.

The spherical composition B surface burst tests were then run for comparison with known TNT results. Spherical composition B charges were also evaluated for the effects of small elevations on the air-blast parameters. The spheres were elevated 3 radii of a cylinder (L/D = 1) of the same weight. Air-blast parameters from cylindrical composition B surface bursts and elevated detonations were measured and used for evaluating shape and elevation effects.

Explosives

The explosives used in testing were cast composition B hemispheres, spheres, and cylinders (L/D = 1) and rigid plastic cylindrical containers of an RDX slurry (RDX in a solution of 60% acetic acid, 38% water, and 2% nitric acid). Dimensions and weights are shown in Figure 1. Table 2 also details the variation in the slurry dimensions, and Figure 2 shows

the two sizes of RDX slurry containers. Charge weights were taken and marked on the charge by the manufacturer. Charge weight variation of the composition B was insignificant (less than 1%). Variation of the RDX slurry weights and dimensions was significant. The thickness of the settled RDX, which solidified at the bottom of the container, varied linearly along diameters through the center of the RDX disc. This resulted when the manufacturer did not place the charges perfectly vertical in their shipping barrels. The weight variation can be allowed for with scaling, but the variation in thickness of the RDX disc at the bottom of the container definitely contributed to greater scatter of the RDX slurry test data.

The composition B charges were cast and machined to accept an Engineers Special (J2) blasting cap. The spherical charge was cast with a 22-gram spherical pentolite booster centered in the sphere. Charge weights shown in Figure 1 do not include the weight of the booster charge or blasting cap except for the spherical charge which was weighed with the booster in place. The composition B charge weights in Figure 1 were used in scaling. However, the 100-gram booster of C4 used with the RDX slurry charges was added to the RDX weight when analyzing those results.

The composition B hemispheres and spheres were cast by the Naval Ordnance Laboratory (NOL), Silver Spring, MD. The composition B cylinders were cast and machined by NOL and by the Naval Weapons Center, China Lake, CA. Holston Army Ammunition Plant made up the RDX slurry charges with slurry taken directly from their manufacturing tanks.

Test Site

Testing was conducted at the Pacific Missile Range, Point Mugu, CA. Three gage lines, each originating at ground zero, were placed at 90 degrees to each other. The ground surface, along each gage line, was leveled and covered out to a range of 52 feet. The first 10 feet of the lines, except for the surface at ground zero, was covered with 4-foot-wide by 1/4-inch-thick steel plate. From 10 to 52 feet, the lines were covered with 3/4-inch plywood. Pressure transducers were located on each line at 2, 4, 8, 16, 32, and 50 feet from ground zero. Each transducer was mounted in a steel jacket encased in 1 cubic foot of concrete. The concrete block was buried so that the pressure gage was flush with the ground surface. Figure 3 shows a gage line and a typical gage mount.

Atmospheric conditions at the site were obtained from the Meteorology Section of the Pacific Missile Range. Barometric pressure, temperature, wind speed, and wind direction are noted hourly from a station within 600 yards of our test site. Meteorological data was included in the computer printout of each pressure record.

Instrumentation

Piezoresistive pressure transducers manufactured by Tyco Instrument Division of Bytrex, Inc. were used. The HFG series gage used is specifically designed to measure blast phenomena in a field test situation. The gage is

Table 1 Summary of Test Program[a]

Explosive			Conditions		Recording System nominal response	Data Source (Ref.)
Composition	Shape	Weight[c] lb	Elevation[b] m	Surface		
TNT	spheres	[illegible]	[illegible]	steel plate	20 kHz	poor detonations, results not shown
		[illegible]	[illegible]	steel plate	20 kHz	
		[illegible]	[illegible]	steel plate	20 kHz	
		[illegible]	6.0	steel plate	20 kHz	
		[illegible]	6.6	steel plate	20 kHz	
		[illegible]	[illegible]	steel plate	20 kHz	
Composition B	cylinders (L/D = 1)	[illegible]	[illegible]	steel plate	20 kHz	9
		[illegible]	4.0	steel plate	20 kHz	
		[illegible]	[illegible]	steel plate	20 kHz	
		[illegible]	5.2	steel plate	20 kHz	
		[illegible]	6.0	steel plate	20 kHz	
[illegible] slurry	[illegible]	[illegible]	5.2	steel plate	20 kHz	10
		[illegible]	6.6	steel plate	20 kHz	
Composition B	hemispheres	[illegible]	surface burst	steel plate and sand	20 kHz	3, 4
		[illegible]			20 kHz	
Composition B	spheres	[illegible]	surface burst and 4.1	steel plate	40 kHz	5, 7
	spheres	[illegible]	surface burst and 5.9	steel plate	40 kHz	
Composition B	cylinders	[illegible]	surface burst and 4.8	steel plate	40 kHz	6, 8
	cylinders	[illegible]	surface burst and 6.0	steel plate	40 kHz	

[a] Shown in sequence of testing.

[b] Elevations from ground to center of gravity of charge except for slurry, which was measured to bottom of container.

[c] Includes weight of [illegible] booster.

supplied with an integral heat and debris shield with eight equally spaced holes of 0.040-inch diameter leading to the gage diaphragm. The filter provides a cylindrical air space above the diaphragm of 0.010 inch. The diameter of the space varies with the pressure range of the gage. Gages designed to measure peak pressures of 15, 25, 100, 200, 500, and 1,000 psi were placed along the gage line in accordance with the predicted pressure at the gage location. Gages were statically precalibrated with air pressure at about the level of the anticipated peak shock pressure. Instrument cables were buried for protection. Recording equipment was housed in a hardened instrument van located 50 feet from ground zero. (The van was originally located 300 feet from ground zero for the nominal 20-kHz recording system, but was moved when the recording system capability was increased to a nominal 40 kHz.)

In the beginning of the test program a nominal 20-kHz recording system was used. This system consisted of Endevco Models 4401 and 4470 signal conditioners, Dana Models 3850V2 and 4472-6 amplifiers, and a Sangamo Saber 4 tape recorder at 60 ips. This system was used for the hemispherical composition B tests, the RDX slurry tests, and a portion of the elevated composition B cylinder tests (Table 1 shows the recording system used in each test).

A nominal 40-kHz recording system was used for the remaining tests. This system substituted Minneapolis-Honeywell Model 104 amplifiers and increased the recording tape speed to 120 ips.

The FM signal data was digitized by the data reduction facility at the Pacific Missile Range. The 20-kHz pressure-time data was digitized at 160 samples per millisecond (6.25 microseconds per data point). The 40-kHz data digitizing rate was doubled to 320 samples per millisecond (3.125 microseconds per data point).

Test Procedure

The test charge was centered on or over ground zero as shown in Figure 4. Charges placed at ground level were positioned on a replaceable 4-inch-thick steel plate. Figure 4a shows a hemispherical charge in place on the steel plate. Elevated* charges were placed on a platform consisting of wooden slats spanning styrofoam cups. Figure 3b shows the simple support for a cylindrical composition B charge, and Figure 4b shows the three-sided support for a heavier RDX slurry charge. The center cup in Figure 4b is supporting a 100-gram C4 booster charge. The blasting cap, which is not visible, was inserted through the cup and into the C4.

Each charge was detonated by an engineers special J2 blasting cap (Navy Ammunition Stock FSN No. 1375-028-5225/4 M130) with a main charge of 0.94 gram of PETN. An additional booster charge was used for each explosive as shown in Figure 1. The hemispherical and cylindrical

---

* Cylinders were elevated 3 radii (ground level to center of gravity); composition B spheres were elevated 3 radii of a cylinder of the same weight; the RDX slurry was elevated 3 radii of a sphere of the same weight (5-3/16 and 6-5/8 inches for the 7 and 8-1/2-inch containers, respectively, ground level to bottom of container).

Table 2. Physical Dimensions of Encased Cylindrical RDX Slurry Charges

Test No.	Weight (lb)		Average Height of RDX (in.)	Height of Slurry (in.)
	RDX[a]	Slurry		
8-1/2-Inch-Diameter Container				
011	3.5	21.1	2-1/16	9-1/2
012	3.6	21.4	2	9
013	3.6	21.5	2	10
030	3.5	20.8	2	10
031	3.5	20.8	2	9-1/2
032	3.6	21.4	2-1/16	10
033	3.6	21.6	2-1/16	9-1/2
034	3.1	18.5	1-13/16	8-3/4
035	3.6	21.6	2-3/16	10
036	3.5	21.0	2-3/16	10 1/2
037	3.3	19.6	2-3/16	9
7-Inch-Diameter Container				
021	1.9	11.3	1-5/8	7
022	1.9	11.1	1-7/16	6-3/4
023	1.8	10.6	1-7/16	6-1/2
024	1.8	10.8	1-7/16	6-3/8
025	1.8	11.0	1-1/2	6-7/8
026[b]	2.0	11.9	1-13/16	7-1/2
027	1.9	11.3	1-5/8	6-7/8
028	2.1	12.0	1-3/4	7-7/8
029	1.9	11.6	1-9/16	6-3/4
020	1.9	11.4	1-5/8	7

[a] Does not include 100-gram booster (C4) weight which is included in scaled distance calculation.

[b] Test not recorded due to instrumentation malfunction.

supplied with an integral heat and debris shield with eight equally spaced holes of 0.040-inch diameter leading to the gage diaphragm. The filter provides a cylindrical air space above the diaphragm of 0.010 inch. The diameter of the space varies with the pressure range of the gage. Gages designed to measure peak pressures of 15, 25, 100, 200, 500, and 1,000 psi were placed along the gage line in accordance with the predicted pressure at the gage location. Gages were statically precalibrated with air pressure at about the level of the anticipated peak shock pressure. Instrument cables were buried for protection. Recording equipment was housed in a hardened instrument van located 50 feet from ground zero. (The van was originally located 300 feet from ground zero for the nominal 20-kHz recording system, but was moved when the recording system capability was increased to a nominal 40 kHz.)

In the beginning of the test program a nominal 20-kHz recording system was used. This system consisted of Endevco Models 4401 and 4470 signal conditioners, Dana Models 3850V2 and 4472-6 amplifiers, and a Sangamo Saber 4 tape recorder at 60 ips. This system was used for the hemispherical composition B tests, the RDX slurry tests, and a portion of the elevated composition B cylinder tests (Table 1 shows the recording system used in each test).

A nominal 40-kHz recording system was used for the remaining tests. This system substituted Minneapolis-Honeywell Model 104 amplifiers and increased the recording tape speed to 120 ips.

The FM signal data was digitized by the data reduction facility at the Pacific Missile Range. The 20-kHz pressure-time data was digitized at 160 samples per millisecond (6.25 microseconds per data point). The 40-kHz data digitizing rate was doubled to 320 samples per millisecond (3.125 microseconds per data point).

Test Procedure

The test charge was centered on or over ground zero as shown in Figure 4. Charges placed at ground level were positioned on a replaceable 4-inch-thick steel plate. Figure 4a shows a hemispherical charge in place on the steel plate. Elevated* charges were placed on a platform consisting of wooden slats spanning styrofoam cups. Figure 3b shows the simple support for a cylindrical composition B charge, and Figure 4b shows the three-sided support for a heavier RDX slurry charge. The center cup in Figure 4b is supporting a 100-gram C4 booster charge. The blasting cap, which is not visible, was inserted through the cup and into the C4.

Each charge was detonated by an engineers special J2 blasting cap (Navy Ammunition Stock FSN No. 1375-028-5225/4 M130) with a main charge of 0.94 gram of PETN. An additional booster charge was used for each explosive as shown in Figure 1. The hemispherical and cylindrical

* Cylinders were elevated 3 radii (ground level to center of gravity); composition B spheres were elevated 3 radii of a cylinder of the same weight; the RDX slurry was elevated 3 radii of a sphere of the same weight (5-3/16 and 6-5/8 inches for the 7 and 8-1/2-inch containers, respectively, ground level to bottom of container).

composition B used boosters of 1/4- by 1/4-inch cylindrical PBXN-5 pellets (about 5 grams) between the charge and the blasting cap. A 22-gram spherical pentolite booster was cast with the spherical charges. A 100-gram truncated cone of C4 booster was centered against the bottom of the RDX slurry containers as shown in Figure 4b.

A programmable sequence control timer activated the recording equipment and detonated the charge. Quick-look data, provided by an oscillograph plotted after each test, allowed correction of instrumentation problems and evaluation of results before continuing the test program.

DATA ANALYSIS

A typical computer printout of a pressure-time and impulse-time data plot is displayed in Figure 5. Peak pressure and maximum impulse were taken directly from this plot of the digitized data. Positive phase duration was found for gages at ranges of 8 feet or further by taking the difference between the times to peak pressure and peak impulse. This was possible since the peak pressure was always the first pressure spike and the initial rise time was small compared to the positive phase duration at these gage locations. At gages 2 and 4 feet from the charge the positive phase was scaled, from the digitized plot, between the start of the leading edge of the pressure curve and the time of maximum impulse.

Gages at ranges of 16, 32, and 50 feet generally exhibited overshoot due to ''ringing'' of the gage diaphragm whose natural frequency was nearly that of the pressure loading. The positive phase duration at these ranges was long enough so that an exponential curve could be fitted through the average of the data points to obtain the correct peak pressure. Since large segments of the exponentially decaying curve will plot as a straight line on a log pressure-versus-time plot [4] these curves were also constructed in some cases to aid in curve fitting. Figure 6 shows the pressure-time plot and a log pressure-time plot for the same record. The peak pressure determined from interpretation of these plots is marked on each sheet. The log pressure plot flattens and straightens the slope of the fitted curve and, thus, allows for better and more consistent peak pressure analysis of ''ringing'' gages. Since the ''ringing'' was balanced around the average pressure-time plot, there was no need to correct the impulse data. Positive phase duration was unaffected by ''ringing.''

The air-blast parameters of peak pressure and scaled unit impulse and scaled positive phase duration are tabulated in Tables 3 through 10. In general the data averages in Tables 3 through 8 are averaged from six readings. Values in Table 9 are the averages of four readings. Values in Table 10 for the 2.1-pound charges are averaged from 18 readings and those for the 3.7-pound charges are averaged from 20 readings. The values in parentheses in these tables are one standard deviation of the data values used to calculate the average.

Testing was done at sea level and meteorological records were kept. However, scaling to sea level conditions [5] was not necessary because the corrections would have been small compared to the standard deviation of the data points.

Table 3. Average Shock Wave Parameters for Hemispherical Composition B Surface Burst on Sand

Charge Weight, W (lb)	Scaled Distance, Z ($ft/lb^{1/3}$)	P_{so} (psi)	$i_s/W^{1/3}$ ($psi\text{-}msec/lb^{1/3}$)	$t_o/W^{1/3}$ ($msec/lb^{1/3}$)
1.0	2.02	177 (14)	16.0 (1.2)	0.28 (0.03)
	4.03	52.4 (5.1)	13.0 (0.5)	1.07 (0.17)
	8.02	13.9 (0.5)	8.20 (0.17)	2.14 (0.21)
	16.0	3.75 (0.16)	4.63 (0.13)	3.09 (0.13)
	32.1	1.33 (0.04)	2.25 (0.03)	3.75 (0.20)
	50.0	0.87 (0.04)	1.55 (0.03)	4.23 (0.19)
2.95	1.41	359 (74)	14.4 (1.0)	0.17 (0.01)
	2.81	99.2 (14.7)	16.9 (0.8)	0.87 (0.30)
	5.59	28.3 (2.6)	10.6 (0.7)	1.69 (0.25)
	11.2	7.13 (0.36)	6.51 (0.16)	2.49 (0.09)
	22.4	2.36 (0.11)	3.19 (0.06)	3.24 (0.06)
	34.9	1.45 (0.09)	2.25 (0.06)	3.88 (0.03)

Table 4. Average Shock Wave Parameters for Hemispherical Composition B Surface Burst on Steel Plate

Charge Weight, W (lb)	Scaled Distance, Z ($ft/lb^{1/3}$)	P_{so} (psi)	$i_s/W^{1/3}$ ($psi\text{-}msec/lb^{1/3}$)	$t_o/W^{1/3}$ ($msec/lb^{1/3}$)
1.0	2.02	242 (17)	17.7 (2.3)	0.32 (0.07)
	4.03	67 (16)	16.0[a]	0.91 (0.11)
	8.02	16.7 (1.4)	9.71 (0.39)	2.82 (0.07)
	16.0	4.29 (0.32)	5.23 (0.24)	3.75 (0.15)
	32.1	1.45 (0.08)	2.41 (0.07)	4.46 (0.25)
	50.0	0.88 (0.09)	1.64 (0.08)	5.17 (0.10)
2.95	1.41	388 (58)	18.5 (0.9)	0.17 (0.04)
	2.81	151 (12)	21.3 (4.4)	1.12 (0.31)
	5.59	31.3 (4.6)	12.8 (0.6)	2.41 (0.14)
	11.2	8.40 (0.70)	7.32 (0.30)	3.28 (0.08)
	22.4	2.50 (0.15)	3.47 (0.14)	3.79 (0.59)
	34.9	1.43 (0.08)	2.34 (0.16)	4.67 (0.25)

[a] Average of only two good measurements.

Table 5. Average Shock Wave Parameters for Spherical Composition B Surface Burst

Charge Weight, W (lb)	Scaled Distance, Z ($ft/lb^{1/3}$)	P_{so} (psi)	$i_s/W^{1/3}$ ($psi\text{-}msec/lb^{1/3}$)	$t_o/W^{1/3}$ ($msec/lb^{1/3}$)
1.07	2.00	468 (102)	19.9 (3.2)	0.12 (0.01)
	3.95	112 (5)	23.8 (1.0)	2.01 (0.25)
	7.85	19.5 (1.4)	10.8 (1.2)	1.96 (0.24)
	15.6	4.99 (0.32)	5.50 (0.13)	3.01 (0.13)
	31.4	1.59 (0.03)	2.55 (0.15)	3.68 (0.07)
	48.9	0.83 (0.03)	1.47 (0.09)	4.41 (0.31)
2.69	1.47	480 (103)	18.8 (0.81)	0.09 (0.01)
	2.90	279 (51)	40.9 (2.6)	1.26 (0.16)
	5.77	39.0 (6.2)	14.1 (1.4)	1.34 (0.15)
	11.5	8.29 (0.39)	7.30 (0.16)	2.48 (0.30)
	22.6	2.57 (0.10)	3.49 (0.23)	3.50 (0.44)
	36.0	1.32 (0.11)	2.08 (0.16)	4.13 (0.23)

Table 6. Average Shock Wave Parameters for Cylindrical Composition B Surface Burst

Charge Weight, W (lb)	Scaled Distance, Z ($ft/lb^{1/3}$)	P_{so} (psi)	$i_s/W^{1/3}$ ($psi\text{-}msec/lb^{1/3}$)	$t_o/W^{1/3}$ ($msec/lb^{1/3}$)
1.49	1.79	725 (119)	25.9 (3.2)	0.09 (0.01)
	3.54	148 (13.2)	28.7 (3.7)	0.91 (0.13)
	7.03	31.9 (4.6)	11.0 (1.3)	1.44 (0.18)
	14.0	5.62 (0.63)	5.70 (0.15)	3.70 (0.46)
	28.1	1.68 (0.12)	2.89 (0.19)	4.18 (0.41)
	43.8	0.86 (0.05)	1.81 (0.15)	4.80 (0.38)
3.03	1.41	921 (130)	22.6 (2.2)	0.08 (0.01)
	2.79	289 (28.8)	40.8 (5.5)	0.87 (0.11)
	5.55	47.8 (2.2)	16.2 (1.8)	1.33 (0.18)
	11.1	9.77 (1.02)	6.60 (0.10)	3.02 (0.88)
	22.2	2.39 (0.13)	3.38 (0.59)	4.35 (0.71)
	34.6	1.18 (0.11)	2.26 (0.28)	4.73 (0.46)

Table 7. Average Shock Wave Parameters for Elevated[a] Spherical Composition B

Charge Weight, W (lb)	Scaled Distance, Z (ft/lb$^{1/3}$)	P_{so} (psi)	$i_s/W^{1/3}$ (psi-msec/lb$^{1/3}$)	$t_o/W^{1/3}$ (msec/lb$^{1/3}$)
1.07	2.00	[b]	26.8 (5.0)	0.32 (0.14)
	3.95	95[c]	17.0 (2.0)	0.80 (0.14)
	7.85	20.6 (2.2)	10.9 (1.7)	2.03 (0.47)
	15.6	4.83 (0.37)	5.46 (0.10)	3.13 (0.39)
	31.4	1.61 (0.12)	2.59 (0.15)	3.57 (0.21)
	48.9	0.84 (0.09)	1.50 (0.12)	4.50 (0.28)
2.69	1.47	[b]	21.8 (3.3)	0.17 (0.07)
	2.90	187 (14)	31.6 (4.1)	1.11 (0.34)
	5.77	40.7 (9.5)	13.6 (2.3)	1.71 (0.10)
	11.5	8.86 (0.40)	7.17 (0.14)	2.33 (0.11)
	22.6	2.60 (0.31)	3.[illegible]9 (0.22)	3.21 (0.18)
	36.0	1.28 (0.13)	2.02 (0.16)	3.84 (0.08)

[a] Elevated so that center of gravity of sphere at same elevation as cylinder of same weight elevated at 3 radii (4.1 and 5.9 inches for 1.07- and 2.69-pound charges, respectively).

[b] Peak pressure attenuated by instrumentation limits.

[c] One measurement.

Table 8. Average Shock Wave Parameters for Elevated Cylindrical Composition B (40-kHz Recording System)

Charge Weight, W (lb)	Scaled Distance, Z (ft/lb$^{1/3}$)	P_{so} (psi)	$i_s/W^{1/3}$ (psi-msec/lb$^{1/3}$)	$t_o/W^{1/3}$ (msec/lb$^{1/3}$)
1.49	1.79	663 (78)	29.4 (2.4)	0.19 (0.07)
	3.54	112 (9.8)	23.3 (1.4)	1.25 (0.09)
	7.03	34.5 (4.3)	12.2 (1.0)	1.50 (0.12)
	14.0	5.82 (0.20)	6.01 (0.13)	4.16 (0.10)
	28.1	1.65 (0.09)	2.97 (0.27)	4.45 (0.61)
	43.8	0.85 (0.09)	1.79 (0.15)	5.25 (0.11)
3.03	1.41	1,213 (143)	25.7 (3.0)	0.13 (0.02)
	2.79	223 (21)	28.0 (2.3)	0.90 (0.30)
	5.55	49.2 (1.7)	14.6 (1.5)	1.06 (0.20)
	11.1	9.19 (0.41)	7.19 (0.17)	3.68 (0.17)
	22.2	2.49 (0.07)	3.66 (0.33)	4.29 (0.35)
	34.6	1.23 (0.12)	2.28 (0.21)	4.98 (0.22)

Table 9. Average Shock Wave Parameters for Cylindrical Composition B Elevated 3 Radii (20-kHz Recording System)

Charge Weight, W (lb)	Scaled Distance, Z (ft/lb$^{1/3}$)	P_{so} [a] (psi)	$i_s/W^{1/3}$ [a] (psi-msec/lb$^{1/3}$)	$t_o/W^{1/3}$ (msec/lb$^{1/3}$)
0.50	2.52	282	31.4	0.64
	5.04	72.4	17.3	1.06
	10.1	11.4	8.51	1.94
	20.2	3.15	4.49	4.52
	40.4	0.96	2.12	5.15
	63.0	0.50	1.35	5.37
1.00	2.0	432	28	0.30
	4.0	116	24.9	0.90
	8.0	24.5	10.0	1.50
	16.0	4.99	5.46	4.08
	32.0	1.31	2.59	4.98
	50.0	0.68	1.65	5.20
1.49	1.75	643	44.1	0.21
	3.50	148	27.6	0.96
	7.00	32.1	11.0	1.25
	14.0	6.31	6.28	3.96
	28.0	1.64	2.97	4.85
	44.0	0.87	2.02	5.23
2.01	1.61	662	43	0.23
	3.18	204	31.3	0.72
	6.36	44.2	13.0	1.14
	12.7	7.90	6.70	3.91
	25.4	1.97	3.22	4.69
	39.7	1.03	2.03	5.04
3.03	1.38	514	40	0.21
	2.78	268	34.5	0.89
	5.56	57.8	15.0	1.15
	11.1	10.9	8.21	3.91
	22.2	2.60	4.14	4.61
	34.8	1.33	2.60	5.00

[a] Average of four test values; standard deviation not shown because of small number of samples.

Table 10. Average Shock Wave Parameters for Elevated RDX Slurry in Cylindrical Containers

Charge Weight,[a] W (lb)	Scaled Distance,[b] Z (ft/lb$^{1/3}$)	P_{so} (psi)	$i_s/W^{1/3}$ (psi-msec/lb$^{1/3}$)	$t_o/W^{1/3}$ (msec/lb$^{1/3}$)
2.1 (0.1)	1.57	472 (79)	38.5 (5.5)	0.34 (0.04)
	3.13	155 (22)	26.8 (2.9)	0.62 (0.15)
	6.26	40.5 (3.0)	14.9 (1.5)	1.24 (0.12)
	12.5	8.27 (0.66)	7.30 (0.49)	2.55 (0.26)
	25.0	2.29 (0.17)	3.46 (0.22)	3.64 (0.20)
	39.1	1.00 (0.08)	1.98 (0.11)	4.13 (0.21)
3.7 (0.2)	1.29	603 (178)	46.2 (5.6)	0.37 (0.05)
	2.59	209 (42)	28.0 (4.5)	0.57 (0.19)
	5.17	55.8 (8.7)	17.8 (1.7)	1.24 (0.13)
	10.3	11.7 (1.1)	8.83 (0.78)	2.12 (0.16)
	20.7	3.07 (0.23)	4.27 (0.28)	3.32 (0.14)
	32.3	1.36 (0.09)	2.44 (0.22)	3.81 (0.20)

[a] Average weight of nine test samples includes weight of composition C4 booster. Value in parentheses is one standard deviation.

[b] Average scaled distances shown. Actual scaled distances varied with charge weight. Standard deviation is less than 2% of average.

Surface Burst Data

Hemispherical Composition B and Ground Effect. Peak pressure and scaled unit impulse results from hemispherical composition B surface bursts, tabulated in Tables 3 and 4, are plotted in Figures 7 and 8. Peak pressure data points are shown with the relationship for a TNT hemispherical surface burst [1 and 6]. The tests conducted on a sand surface are generally lower than those detonated over a steel plate. This effect diminishes as the scale distance (Z) increases and is insignificant for Z greater than 20 ft/lb$^{1/3}$.

The same effect is also apparent in the impulse data (see Figure 4) in which the effect of the sand surface is to reduce the scaled unit impulse over the entire range of measured values. The greatest effect is again at the closest ranges.

Because the sand surface obviously reduced the air blast output significantly it was decided that all subsequent surface burst tests would be conducted on a stiff steel plate.

The peak pressure output of the composition B (on a steel plate) is virtually the same as that for a similar TNT charge to a scale distance within 3 ft/lb$^{1/3}$ of the charge. Inside this scale distance the reduced values from our tests of the composition B are most likely due to limitations in the nominal 20 kHz pressure recording system. Because of this attenuation in peak pressure, a nominal 40 kHz recording system was installed for subsequent tests (see Table 1 for the recording system used in each test series).

Scaled impulse data usually shows more scatter than peak pressure data. A comparison of composition B hemispherical surface burst data (on a plate) and two sources of TNT data for similar conditions [1, 6] is of interest in Figure 8. Our test results for composition B show good agreement with those of Kingery [6] who gives measurements of air blast from 5, 20, 100, and 500-ton TNT hemispherical surface bursts. The largest discrepencies occur at scaled distances less than 3 ft/lb$^{1/3}$ where the peak pressures were attenuated by our recording system.

Positive phase durations from the composition B tests and from References 1 and 5 are compared in Figures 17 and 18. The large scatter in our test data around $Z = 4$ ft/lb$^{1/3}$, which shows in the standard deviation and in the erratic data points, is due to the definition of the positive phase used in evaluating our data. Since the positive phase was taken to the time of the peak impulse, it sometimes was extended by low pressure reflection waves. Inspection of Figure 5 will show a second rise in the impulse curve due to a pressure spike at about 6.8 milliseconds elapsed time. In some cases (especially at $R = 4$ feet) this pressure spike caused the second impulse peak to be higher than the first peak and extended the positive phase duration. Again, the data values compare better with Reference 6 than Reference 1.

Spherical Composition B. Peak pressures, scaled unit impulses and scaled positive phase durations for spherical composition B surface bursts are tabulated in Table 5. The peak pressure data is compared in Figure 9 to large TNT test data from Distant Plain Event 6 [7] and Prairie Flat [8, 9]. Curves from the TNT tests had been adjusted to sea level conditions. The 40-kHz recording system appears to increase the acceptable range of the instrumentation to 300 psi (from 150 psi for the 20-kHz system). Below 300 psi the peak pressures from the spherical composition B tests fall on one or the other of the referenced spherical TNT data.

A best fit curve has been drawn through the spherical composition B peak pressure data and compared to hemispherical data in Figure 10. As expected the spherical peak pressures are higher than those of the hemispherical charges at scaled distances less than 15 ft/lb$^{1/3}$. This figure will also be used to determine shape equivalency.

Scaled impulse results, in Table 5, are plotted in Figure 11. A smooth curve has been drawn through the composition B test data for comparison with the large scale TNT data from Distant Plain, Event 6 (100-ton spherical TNT surface burst). Another TNT large-scale surface burst, Operation Prairie Flat, is shown in [8] to be in general agreement with Distant Plain although it is somewhat lower at the larger scale distances

(which puts it closer to the composition B test data). Considering the scatter between like tests of large TNT spheres the composition B spherical surface burst data agrees quite well with results from spherical TNT tests.

Positive phase duration data points from the composition B tests are plotted and compared to results from TNT tests in Figure 17. The composition B data is lower at the larger scale distances and higher at one point near 4 ft/lb$^{1/3}$ scaled distance. The differences are small considering the small effect on the design loading that they would have.

Cylindrical Composition B. Peak pressures, scaled unit impulses and positive phase durations for cylindrical surface bursts are given in Table 6. Average peak pressures are plotted in Figure 12 and connected with a smooth curve. The relationship for a hemispherical TNT surface burst [1] is also shown for comparison when shape equivalencies are calculated. The tabulated values for pressures above 300 psi (Z less than 2.8) were not plotted since the data acquisition system (nominal 40 kHz) was attenuating the peaks in that range.

Peak scaled unit impulses are plotted and connected with a smooth curve in Figure 13. Values are also shown for gages that had attenuated the peak pressure, since the effect on impulse would be much less than that on peak pressure.

Scaled unit positive phase durations are plotted in Figure 18. The relationship for a TNT hemispherical surface burst from Reference 1 is included for comparison.

Effect of Small Heights of Burst

The RDX slurry tests had originally been detonated at small elevations to reduce cratering and simplify the test setup. They were to be compared directly to TNT spheres at the same elevation until improper detonation of the TNT charges made that impossible. Composition B cylinders and spheres were detonated at small heights of burst to see how the results differed from those of surface bursts. The cylinders were elevated 3 radii (ground surface to center of gravity of charge) and the spheres 3 radii of a cylinder of the same weight. Table 1 summarizes the heights of burst for the different charges. Tables 7 and 8 summarize the results for the spheres and cylinders, respectively.

Peak pressures and scaled unit impulses for the elevated spheres and cylinders are compared in Figure 14. Data points from the elevated tests are plotted with the best fit curves from the surface burst tests. Small differences in peak pressure occur at levels above 100 psi with the elevated results being slightly lower. Elevating the charges appeared to reduce the peak that occurs in the impulse relationship at a scaled distance of about 3 ft/lb$^{1/3}$.

Changes in scaled positive phase duration also occur at scaled distances less than 5 ft/lb$^{1/3}$, as can be seen by inspection of Tables 6 and 8. At scaled distances less than 2 ft/lb$^{1/3}$, the duration was increased significantly. (It should be noted that the distances used were measured along the ground surface and were not slant distances from the center of the charge.)

The data shown in Table 9 is for elevated cylinders. It was run at the beginning of the test program along with the TNT spheres (that exhibited poor detonation and are not shown) and the RDX slurry. Subsequent to those tests the test plan was changed to increase the response of the recording system. Since the elevated cylinder tests were essentially repeated (see Table 8) with a better instrumentation system the data in Table 9 is not used in the data plots. It is included, however, to show that it differs only slightly from the latter data to lend credence to the RDX slurry results from the same 20-kHz recording system.

RDX Slurry

Peak pressures, scaled unit impulses and positive phase durations from the RDX slurry tests are summarized in Table 10. Peak pressure data values are plotted and connected with a smooth curve in Figure 15. Peak pressures above 200 psi were not used because of the limitations of the instrumentation above this level. Some reduction in peak pressure (from that of a surface burst) can also be expected above 100 psi, since the charges were elevated (see previous section). The TNT surface burst curve for a hemisphere [1] is also shown for comparison and for use in figuring an equivalency.

Peak scaled unit impulse values are plotted in Figure 16. The significant feature of the curve is that it shows no peak near a scaled distance of 3 ft/lb$^{1/3}$ as did the other tested charges. Instead it continues to rise at a reduced rate.

Scaled positive phase duration for the RDX slurry is plotted in Figure 18 with the relationship for a TNT hemispherical surface burst [1] for comparison.

Three-Wall Cubicle Effects

Peak pressure, scaled impulse, and scaled duration data around a three-wall cubicle were obtained from 1-pound spheres and cylinders and 2.65-pound spheres centered in the cubicle. Gage lines were located along the ground surface perpendicular to the front (open) wall, the sidewall, and the backwall. Data from the two charge shapes of the same weight (1 pound) and from two charge weights of the same shape (spherical) are compared in the Test Results section of this report.

TEST RESULTS

Hemispherical and spherical composition B surface burst tests were conducted for comparison with the latest TNT data for the same shapes and conditions. These tests provided the basis for evaluating the cylindrical composition B and RDX slurry test data by giving a check on the data acquisition system and by yielding the TNT equivalency of composition B. The concept of equivalency is then used to describe the effect of charge

shape (cylinder, sphere and disc versus a hemisphere) on air-blast parameters.

The equivalent weight concept provides a method for comparing air-blast parameters of dissimilar charges. It is most advantageous if it is constant over wide ranges of scaled distance, as it is now presented in TM5-1300. Equivalency by weight is defined as the ratio of the weights of two dissimilar charges that give the same peak pressure (or impulse) at the same range from ground zero. This equivalency can be obtained for peak pressure from pressure versus scaled distance relationships by raising the ratio of the scaled distances, at a constant pressure, to the third power.

$$\left(\frac{Z_x}{Z_y}\right)^3 = \left(\frac{R/W_x^{1/3}}{R/W_y^{1/3}}\right)^3 = \frac{W_y}{W_x} \quad \text{at constant pressure, } P_{so}$$

This equivalency (W_y/W_x) can be plotted against pressure, Z_x or Z_y, since all three define a unique condition where the equivalency applies. In this report the equivalency values are plotted against Z_x since the designer will generally know R and W_x and be looking for W_y.

The impulse equivalency by weight is obtained from scaled impulse versus scaled distance curves by cubing the ratio of scaled distances that fall on lines of constant impulse (psi-msec). On a log-log plot of scaled impulse (psi-msec/lb$^{1/3}$) versus scaled distance (ft/lb$^{1/3}$), impulse (psi-msec) is constant along lines with a slope of 45 degrees. On these lines:

$$i/W^{1/3} = a(R/W^{1/3})^{1.0}$$

or

$$i = aR$$

where a is a constant that locates the 45-degree line. Thus, along these lines the conditions for equivalency are satisfied; that is, impulse and range are constant.

TNT Equivalency of Composition B

The composition B hemispherical and spherical surface burst data is compared to data from similar tests of larger quantities of TNT in Figures 7, 8, 9, and 11. Differences are small or explainable.

Peak pressure from the hemispherical composition B surface burst, detonated on a plate, is virtually the same as that from TNT (see Figure 7), except for peak pressures above 150 psi. Peak pressure levels above the 150-psi level were determined to be low because of the limits of the recording system. Similar results were obtained with a sphere; the composition B test values fall on one or the other of the TNT curves (see Figure 9), except for pressures above 300 psi where the improved (40-kHz) recording system attenuated the peak pressure.

Scaled impulse from composition B and TNT hemispherical surface bursts are compared in Figure 8. Agreement between the composition B data (on a steel plate) and Kingery's TNT data [6] is good. The impulse curve in TM5-1300 [1] is higher and also smooths the peak in the curve at about 2.5 ft/lb$^{1/3}$. Since TM5-1300 references Kingery's report, it must be assumed that the curve in TM5-1300 is the result of a generally conservative smoothing of the relationship over a wide range of scale distances for easier presentation and use. Subsequent references to hemispherical TNT impulse data will refer to Kingery's data.

It was anticipated that composition B and TNT charges of the same shape and under similar conditions would have almost identical blast yield. TM5-1300 gives the TNT equivalencies for composition B at pressures between 2 and 50 psi as 1.10 for peak pressure and 1.06 for impulse. In order to measure these equivalencies experimentally you must be able to measure a ratio in the scaled distances, at the same pressure or impulse, of 1.03 ($1.10^{1/3}$) and 1.02 ($1.06^{1/3}$), respectively. Determining such a low equivalency was not possible because of (1) the magnitude of the standard deviation and (2) the relatively small number of data points. It is important to note that the standard deviation reflects natural differences between identical tests as well as experimental error. The difference between Distant Plain Event 6 and Prairie Flat, shown in Figure 9, is an example. At the lower pressure levels the two similar tests differ by more than 10%. This difference can be attributed to many factors including blast anomalies, test site differences, and experimental error. A series of tests on the same site eliminates the effect of different test site conditions. However, when the results are applied to a situation at another location, this error reenters.

Within the accuracy of the test setup, differences between composition B and TNT peak pressures and scaled impulse for similar shapes were negligible. Considering the natural variation of explosive yields and the compromises necessary by a designer, composition B and TNT can be considered to have the same pressure and impulse outputs. Other factors, such as surface conditions and charge shape, are more important. To be conservative, the TNT equivalencies in TM5-1300 can be applied to composition B.

The results of the hemispherical and spherical composition B surface bursts also verify the accuracy of the instrumentation system. Pressure data from the 20-kHz system is good to 150 psi and from the 40-kHz system to 300 psi. Impulse data is accurate over the entire range of scaled distances, even though it may be slightly low at pressure ranges above the pressures at which the peak is attenuated.

Shape Equivalency

It is recognized that charge shape has a significant effect on airblast parameters. Results from charges of numerous shapes, reported by Adams, et al. [10] in 1949, showed the effects. The data, however, was limited to pressures between 2 and 11 psi. Recent studies of cylinders, spheres, and hemispheres provide data over a much greater pressure range and show the equivalency to be variable with scaled distance.

Air-blast measurements from spherical and hemispherical surface bursts are well documented. The peak pressure from a spherical charge is about twice that of a hemispherical charge at a scaled distance of 2 ft/lb$^{1/3}$ [7]. The pressure curves of the two shapes are shown [7] to merge at scaled distances greater than 10 ft/lb$^{1/3}$. Scaled impulse data is identical [7] for the two shapes at scaled distances greater than 6 ft/lb$^{1/3}$. At a scale distance near 3 ft/lb$^{1/3}$ the scaled impulse from a sphere is about 1.5 times that of a hemisphere. Though these are the maximum differences in peak pressure and impulse, they illustrate the great effect of charge shape at specific scaled distances.

Air-blast measurements from cylindrical charges with various length to diameter (L/D) ratios have been reported by Wisotski and Snyer of the Denver Research Institute [11] and by Reisler and LeFevre [12] of BRL. Their comparisons of cylinders (with L/D ratios between 1 and 3) and spheres have shown that cylinders produce higher pressures (up to 40% higher for an L/D = 1) at scaled distances less than 10 ft/lb$^{1/3}$ and lower pressures (up to 20% lower) at larger scaled distances.

Peak pressure measurements were compared in these references by taking their ratio at given scaled distances. An alternate method would be to show the ratio of equivalent weights that produce the same pressure (or impulse) at the same ground range.

<u>Pressure Equivalency.</u> Peak pressures from hemispherical, spherical, and cylindrical surface bursts are compared in Figure 19. The spherical and cylindrical curves are from composition B test results. The hemispherical relationship is taken from TM5-1300 for a TNT surface burst though the composition B results can be considered identical (see TNT equivalency of composition B, this report). Equivalent weight ratios for pairs of charges of different shape are shown in Figure 20. As expected the weight of a hemispherical charge (W_{hem}) must be greater than that of a sphere (W_{sph}) or cylinder (W_{cyl}) to produce the same pressure at the same near field range. The opposite is true, but to a smaller degree, at the far field ranges. The composition B test data was limited to a minimum scaled distance of 2.80 ft/lb$^{1/3}$. Data from Reisler [7] indicated that the equivalent weight of a hemisphere to that of a sphere ''peaks'' at 3.25 lb/lb at a scaled distance of 2 ft/lb$^{1/3}$. Data is not available at the small scaled distances to determine the peak equivalency for the cylinder.

The high equivalency values are not unusual. The basic pressure curves for spheres and hemispheres are well documented but are not usually compared in this manner. Since pressure (and impulse) changes are relatively insensitive to weight changes ($Z \div 1/W^{1/3}$), equivalent weights amplify the pressure (or impulse) differences. (Note that at a scaled distance of 2 ft/lb$^{1/3}$ the peak pressure of a sphere is about twice that of a hemisphere, but the equivalent weight of the hemisphere to produce that pressure is 3.25 times the weight of a sphere).

<u>Impulse Equivalency.</u> Scaled unit impulses from hemispherical, spherical, and cylindrical surface bursts are compared in Figure 21. The spherical and cylindrical curves are from the composition B test results.

The hemispherical relationship is taken from Kingery's [6] TNT data. The hemispherical composition B results were in good agreement with the TNT results (Figure 8). The TNT data was used since it is a composite of many large scale tests and since the differences between TNT and composition B are not measurable within the accuracy of our recording system. Thus, the effect of charge shape on impulse is the result (whether the curve is based on TNT or composition B). Considering the scatter of impulse data, the only significant differences occur at scale distances less than about 6 ft/lb$^{1/3}$. The scaled impulses of the cylinder and sphere peak much higher than the hemisphere (42 versus 26 psi-msec/lb$^{1/3}$) and at a slightly larger scaled distance. The data also shows the usual trend of scaled impulse data to fall from the peak value (near 3 ft/lb$^{1/3}$) until it again increases with decreasing scaled distance.

Because of the slope reversal in the impulse data near a scaled distance of 3 ft/lb$^{1/3}$, there is a discontinuity in equivalent weights. (Equal impulse lines are at a 45-degree slope on the scaled impulse versus scaled distance plots. Pairs of scaled distance values that fall on these 45-degree lines describe the weight equivalency. A point by point analysis results in a discontinuity when the impulse curve reverses slope to one greater than 45 degrees. This occurs at the peak of the lower curve when values are being calculated point by point at decreasing scaled distances.) For this reason the impulse equivalency curve in Figure 22 for W_{hem}/W_{cyl} is terminated at 3.2 ft/lb$^{1/3}$. Results for a sphere (W_{hem}/W_{sph}) would have been similar within the same range of scaled distances.

Equivalency of RDX Slurry

The RDX slurry peak pressure and scaled impulse data is compared to TNT hemispherical results in Figures 15 and 16. The TNT pressure data was taken from TM5-1300 [1] and the impulse data from Kingery [6]. The equivalent weight ratios (W_{TNT}/W_{slurry}) were calculated from these figures and are displayed in Figure 23. The pressure equivalency is highest (1.80 lb/lb) at a scaled distance of 5.2 ft/lb$^{1/3}$. The impulse equivalency is between 1.3 and 1.4 lb/lb for scaled distances between 2.7 and 10 ft/lb$^{1/3}$. Inspection of Figure 16 shows that at a scaled distance near 2.7 ft/lb$^{1/3}$ a discontinuity in impulse equivalency occurs. At scaled distances less than 2.6 ft/lb$^{1/3}$ the equivalency increases substantially to a value of around 5 lb/lb. This high equivalency occurs because the impulse curve for the RDX slurry does not exhibit the trend of impulse data from other charges to turn down at a scale distance around 3 ft/lb$^{1/3}$ before again increasing with decreasing scaled distance.

The equivalency values for the RDX slurry indicate that it must be considered as a high explosive with at least the yield of TNT. The variable equivalencies determined in these tests are more indicative of charge shape and type of containment than with equivalency between explosives only differing in composition.

Three-Wall Cubicle Effects

Effect of Charge Shape on Leakage Environment. Pressure gage measurements outside a three-wall cubicle without a roof are presented in Tables 11 and 12, showing blast environment from 1-pound cylindrical and spherical charges. Results from pressure gages outside the open front wall of the cubicle are shown in Figure 24. Charge shape did not affect scaled durations at any scaled distance. At scaled distances greater than 4 ft/lb$^{1/3}$, scaled impulse and peak pressure data showed no charge shape effects. The average peak pressure of the cylinder at 4 ft/lb$^{1/3}$ was 15% higher than that of the sphere and the scaled impulse of the cylinder at 2 ft/lb$^{1/3}$ was 14% higher than that of a sphere. Cylindrical charge data on a line perpendicular to the open wall of a cubicle can be used for predicting the environment from spherical charges. At worst, the data will be slightly conservative at scaled distances less than 4 ft/lb$^{1/3}$.

Pressure gage measurements along a line perpendicular to the sidewall (Figure 25) followed the same trend as out the front. However, pressures and impulses were affected to a greater scaled distance (8 ft/lb$^{1/3}$). (Note that the cylindrical pressure at 4 ft/lb$^{1/3}$ is higher than the average of numerous tests run during the subsequent cubicle test program. The average from a larger sampling gives a pressure about 20% higher than that of a sphere [2]. Thus, if data from cylindrical charges is used to design for spherical charges, it would be conservative at scaled distances less than 8 ft/lb$^{1/3}$.)

A somewhat different trend is found in comparing results from the sphere and cylinder over the backwall of the cubicle (Figure 26). Scaled durations are still the same. However, spherical pressure data is higher at scaled distances less than about 13 ft/lb$^{1/3}$ and cylindrical impulse data is higher over the entire range of measurements. Thus, impulse data but not pressure data from cylindrical tests can conservatively be used for a spherical charge. However, more extensive testing from three different cylindrical charge weights [2] showed that the peak pressure versus scale distance curve of the cylinder has the same maximum pressure value as that of the sphere but at a closer scaled distance. Because the maximum pressure behind the backwall was the same for both shapes, the design method proposed in Reference 2 is applicable to both. That method uses two intersecting straight lines to describe the pressure environment. A horizontal line (dependent on charge density, W/V) limits the maximum pressure and intersects a diagonal line describing the lower pressures at larger scale distances.

Effect of Charge Weight on Leakage Environment. Two spherical charge weights (1.07 and 2.65 pounds) were tested in the cubicle. Results, presented in Tables 12 and 13 and plotted in Figures 27, 28, and 29, show considerable differences in the blast environment parameters. This is expected since the size of the cubicle remained constant and was not scaled up for the increased charge weight. Correct scaling requires that the charge density, W/V, remain constant. Therefore, results from different charge weights within a single geometry cubicle are dependent on W/V.

Table 11. Blast Pressure Environment Outside Three-Wall Cubicle From 1.00-Pound Cylindrical Charge

Scaled Distance, $R/W^{1/3}$ (ft/lb$^{1/3}$)			Peak Pressure, P_{so} (psi)			Scaled Duration, $t_o/W^{1/3}$ (msec/lb$^{1/3}$)			Scaled Impulse, $i_s/W^{1/3}$ (psi-msec/lb$^{1/3}$)		
Front	Side	Back	Front	Side	Back	Front	Side	Back	Front	Side	Back
2.08	--	1.96	279.0 224.0	-	--	1.62 1.36	-	- -	56.4 37.1	- --	-- -
4.06	4.00	4.08	109.0 121.0	21.8 26.4	7.00 8.49	1.55 1.92	3.30 3.35	5.3 5.1	34.5 38.4	13.5 13.7	9.99 9.01
8.04	7.94	8.05	26.5 28.4	11.6 13.0	5.84 7.67	2.00 1.80	3.40 3.40	5.25 5.15	20.2 20.4	10.6 10.9	8.45 7.90
16.0	15.9	16.0	8.60 8.70	4.63 4.88	4.35 4.40	3.10 3.21	3.80 3.73	5.40 5.60	10.4 10.4	6.65 6.85	5.80 5.40
32.1	32.1	32.1	2.73 2.73	1.85 1.87	1.69 1.71	3.75 3.94	4.20 4.06	5.93 6.46	4.58 4.81	4.04 4.10	3.26 3.16
50.0	50.0	50.0	1.44 1.44	1.14 1.07	0.80 --	5.32 5.17	5.02 4.84	6.18 -	3.02 3.15	2.58 2.54	2.24 -

Table 12. Blast Pressure Environment Outside Three-Wall Cubicle From 1.00-Pound Spherical Charge

Scaled Distance, $R/W^{1/3}$ (ft/lb$^{1/3}$)			Peak Pressure, P_{so} (psi)			Scaled Duration, $t_o/W^{1/3}$ (msec/lb$^{1/3}$)			Scaled Impulse, $i_s/W^{1/3}$ (psi-msec/lb$^{1/3}$)		
Front	Side	Back	Front	Side	Back	Front	Side	Back	Front	Side	Back
			377.0	–	10.2	1.47	–	–	46.3	–	8.90
2.08	–	1.96	341.0	–	9.34	1.49	–	–	31.4	–	9.10
			358.0	–	–	1.56	–	–	45.8	–	–
			107.0	12.8	9.33	1.80	3.15	5.0	37.5	11.4	8.5
4.06	4.00	4.08	97.0	13.5	9.59	1.70	3.10	5.15	32.7	11.4	8.6
			94.0	15.4	9.9	1.75	3.65	4.70	36.3	12.0	9.6
			25.1	11.1	9.15	1.80	3.4	5.05	20.4	10.7	6.8
8.04	7.94	8.05	27.3	11.9	9.17	1.85	3.4	5.00	24.3	10.8	6.7
			30.5	10.7	9.0	1.80	3.4	5.1	21.5	12.0	7.9
			9.35	4.68	4.17	3.04	3.53	5.40	11.1	6.9	4.11
16.0	15.9	16.0	9.18	4.68	3.95	3.15	3.35	5.85	11.1	6.7	4.87
			9.73	4.83	4.29	3.11	3.20	5.62	11.9	7.05	5.05
			2.80	2.17	1.58	3.90	4.04	6.58	4.97	3.88	2.64
32.1	32.1	32.1	2.72	1.94	1.64	3.90	4.00	5.87	4.85	3.87	2.68
			2.83	2.09	1.64	3.83	3.99	6.24	4.88	4.09	2.88
			1.46	1.16	–	5.02	4.84	–	3.15	2.52	–
50.0	50.0	50.0	1.48	1.16	–	5.00	4.73	–	3.13	2.49	–
			1.46	1.19	–	5.10	4.70	–	3.19	2.55	–

Table 13. Blast Pressure Environment Outside Three-Wall Cubicle From 2.65-Pound Spherical Charge

Scaled Distance, $R/W^{1/3}$ (ft/lb$^{1/3}$)			Peak Pressure, P_{so} (psi)			Scaled Distance, $t_o/W^{1/3}$ (msec/lb$^{1/3}$)			Scaled Impulse, $i_s/W^{1/3}$ (psi-msec/lb$^{1/3}$)		
Front	Side	Back	Front	Side	Back	Front	Side	Back	Front	Side	Back
		1.42			24.3			3.11		--	13.4
					25.2			2.97		-	13.7
	2.89	2.95		25.6	16.6		2.46	3.32		12.6	13.3
				18.9	17.3		2.46	3.29		12.9	13.8
5.81	5.74	5.82	44.0	18.5	15.5	1.58	2.67	3.45	23.1	12.2	10.1
			43.1	20.0	16.0	1.55	2.49	3.50	23.5	12.6	10.3
11.6	11.5	11.6	16.9	7.56	6.40	2.38	2.53	4.15	12.6	7.85	6.85
			16.6	8.20	6.20	2.31	2.35	4.00	12.4	8.15	6.95
23.2	23.2	23.2	4.18	2.92	2.41	3.29	3.17	4.15	5.75	4.57	3.56
			4.20	3.00	2.42	3.21	3.24	6.24	5.80	4.53	3.51
36.1	36.1	36.1	2.05	1.72	1.17	4.22	4.20	5.22	3.65	3.17	2.16
			2.10	1.65		4.23	4.11		3.69	3.04	-

CONCLUSIONS

1. The blast environment from composition B charges is essentially equivalent to that from TNT charges of the same shape. The TNT equivalencies in TM5-1300 (1.10 for peak pressure and 1.06 for impulse) should be used in design.

2. The contained RDX slurry used in this test program is a high explosive with a TNT equivalency that varies with scaled distance. The measured equivalencies are more indicative of charge shape and containment effects than the difference in charge composition. Peak pressures and impulses for RDX slurry tanks should be obtained directly from the plots of these parameters versus scaled distances (Figures 15 and 16). Since TNT equivalency by weight is not constant, it offers no advantages in design applications.

3. Charge shape effects on the surface burst environment were substantial at scaled distances less than 20 $ft/lb^{1/3}$. Charge shape must, therefore, be considered at these scaled distances.* Use of data from cylindrical charges at less than 20 $ft/lb^{1/3}$ would be conservative in most cases (that is, charges approaching spherical, hemispherical, or cylindrical shapes).

4. Charge shape changes cause less variation in the blast environment outside a protective cubicle than they do in the case of a surface burst. Use of cylindrical charges for the test program described in Reference 2 will produce design curves that will be applicable for most charge shapes.

5. An extreme difference in surface hardness has significant effect on the surface burst environment at scaled distances less than 20 $ft/lb^{1/3}$. A stiff steel plate on sand, for the scale model tests, gave good agreement with large scale results.

6. Small heights of burst (0.40 $ft/lb^{1/3}$) measurably reduced side-on overpressure and impulse at scaled distances less than 5 $ft/lb^{1/3}$.

RECOMMENDATIONS

Equivalent weights are easy to apply when they are constant over a wide range of scaled distances. However, an equivalency that varies with scaled distance is not practical for design work. Two curves must be used:

* The TM5-1300 Design Manual was developed from tests of TNT and composition B charges of both spherical and cylindrical (L/D = 1) configurations. The design data presented reflects this charge shape phenomenon. For charges with L/D greater than one, a procedure whereby the charge is assumed to consist of a series of spherical charges is used. This procedure has produced good agreement with available test data, and a supplement to TM5-1300 is being prepared.

the variable equivalency plot to determine the equivalent weight of the standard and the applicable parameter curve of the standard. Since the effect of charge shape on air blast is a function of scaled distance, instead of providing a variable equivalency plot the actual air-blast parameter curve for that charge shape should be provided for design. There would be less chance for error and, in the case of impulse relationships, no ambiguous discontinuities.

The shape effects on surface bursts cannot be applied directly to external pressures from a charge confined in a cubicle. However, these tests have demonstrated that results from cubicle tests using composition B cylinders can be safely used for most compact charge shapes. Design curves from Reference 2 can be applied to a wide range of standard charge shapes without correction. This is possible because the cylinder generally gives conservative results (design curves in Reference 2 will allow for the one condition where the cylinder gave lower pressures), and the cubicle wall interference with the blast wave reduces charge shape produced variations in the blast waves.

ACKNOWLEDGMENTS

Mr. Richard Rindner of Picatinny Arsenal conceived and administered the study. Mr. Norval Dobbs of Ammann and Whitney provided valuable technical guidance during the program. Testing was conducted at the Pacific Missile Range, Point Mugu, California. The test site was constructed and maintained by Mr. Vince Gerwe and Mr. David Corrente, CEL Structural Engineering Technicians. Mr. Dale Johnson, CEL Instrumentation Engineer, and Mr. Gerry Duffy, Electronics Technician, designed, installed, and operated the instrumentation system. Handling and detonation of explosives was supervised by Mr. Paul R. Smith of PMR Operations Department, Launching Division.

Data channels were digitized and plotted at PMR by the Data Automation Division. Mr. Larry Fuller and Mr. Tom Morris were especially responsible for the outstanding support from PMR in digitizing over 1,000 data channels and generating over 2,000 data curves in this program.

The author gratefully acknowledges these people and their associates for their contributions to the study.

(a) Hemispherical Charges – Composition B

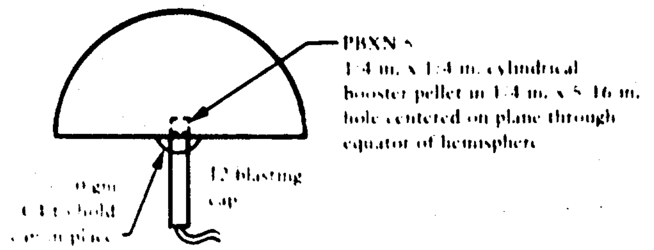

Avg. Charge Weight (lb)	Nominal Diameter (in.)
1.00	4.00
2.98	5.75

(b) Spherical Charges – Composition B

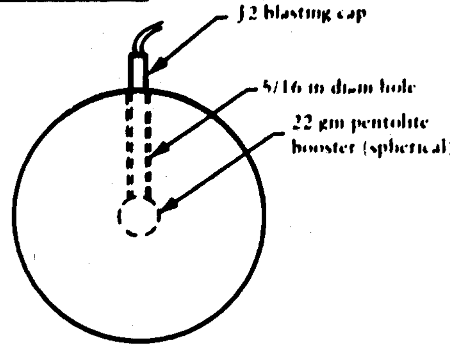

Avg. Charge Weight (lb)	Nominal Diameter (in.)
1.07	3.25
2.69	4.38

(c) Cylindrical Charges – Composition B

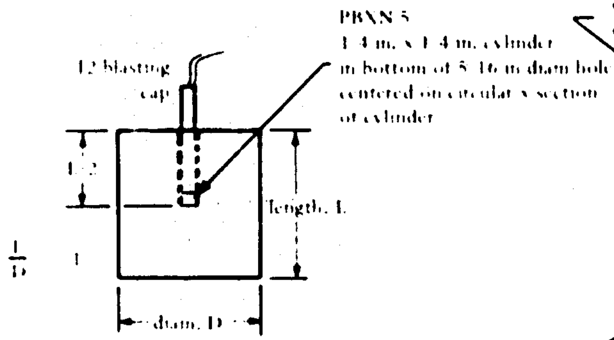

Avg. Charge Weight (lb)	Avg. Diameter (in.)
0.49	2.2
1.00	2.7
1.49	3.2
2.01	3.5
[illegible]	4.0

(d) Encased RDX Slurry Charges*

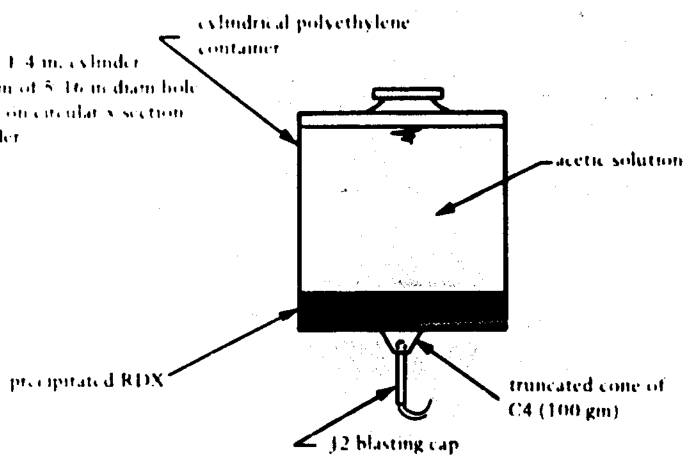

Avg. Charge Weight (lb)	Container Diameter (in.)
1.9	7
3.5	8.5

* See Table 1 for detailed listing of RDX slurry specimen dimensions and Figure 2 for photographs of the slurry specimens.

Figure 1. Charge dimensions.

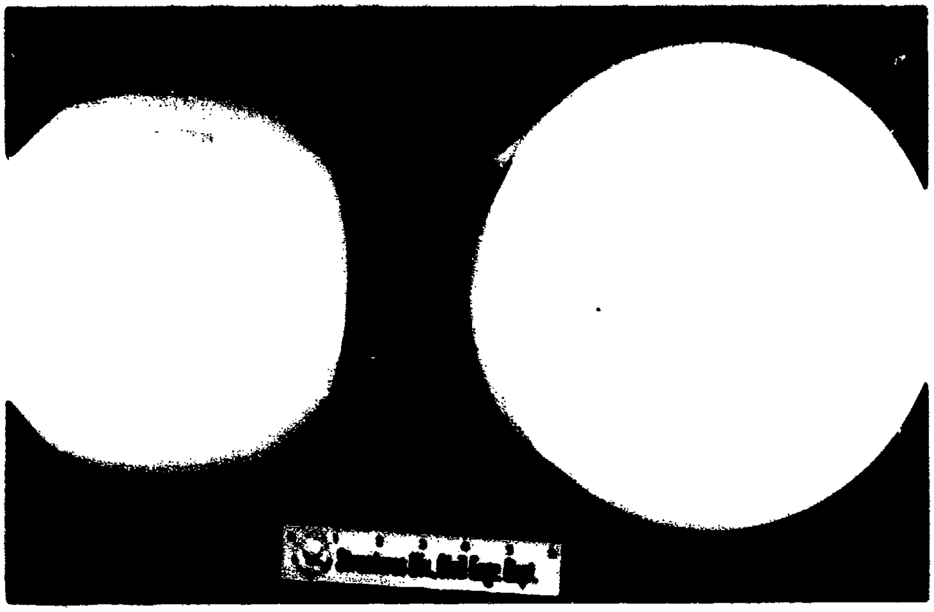

(a) Top view.

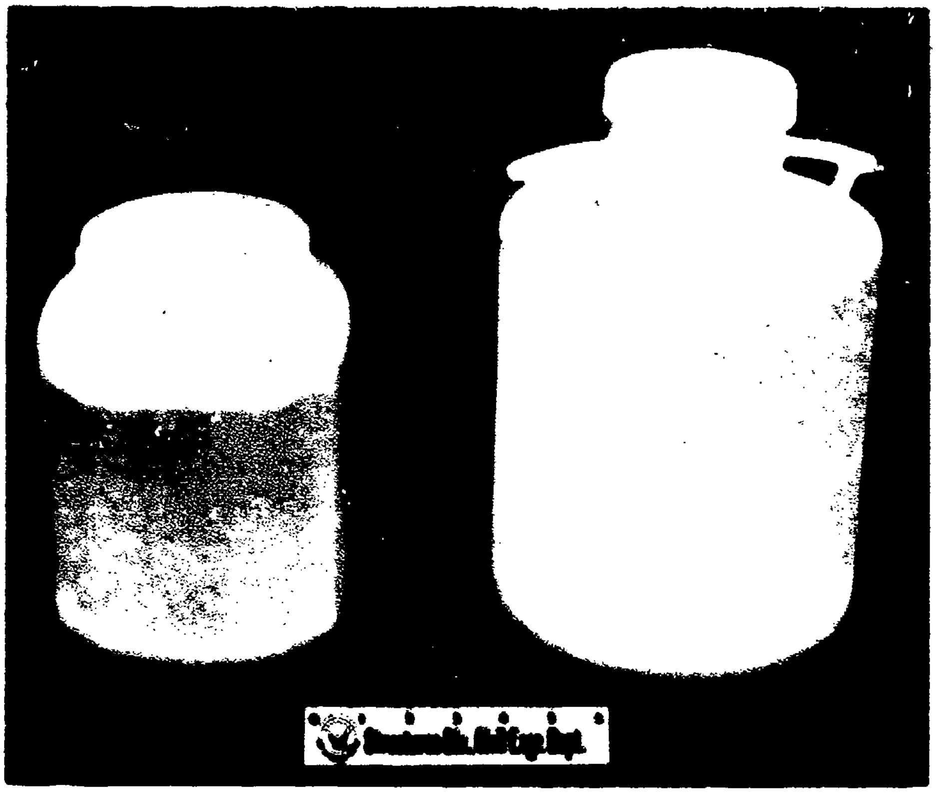

(b) Side view.

Figure 2. RDX slurry test charges of 7- and 8-1/2-inch diameter.

(a) Gage mount (mass provided by 1 foot of concrete).

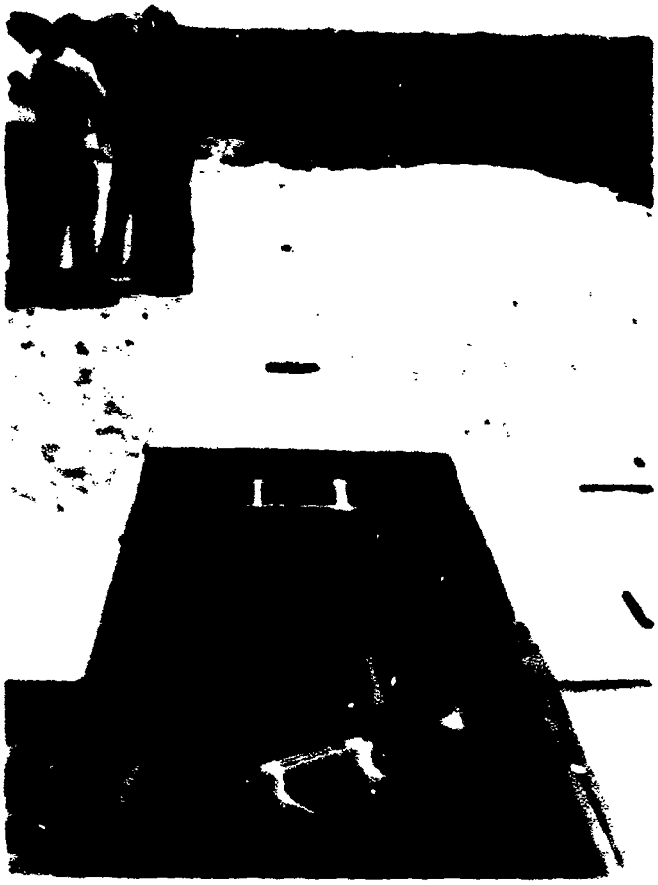

(b) Pressure transducers at 2, 4, 8, 16, 32, and 50 feet from charge.

Figure 3. South gage line of test site.

(a) Surface burst of 2.95-pound hemispherical charge setup on 4-inch steel plate.

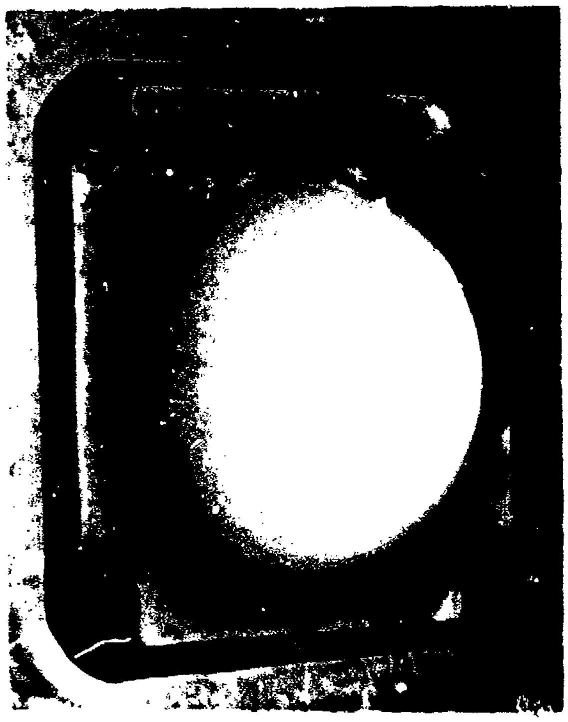

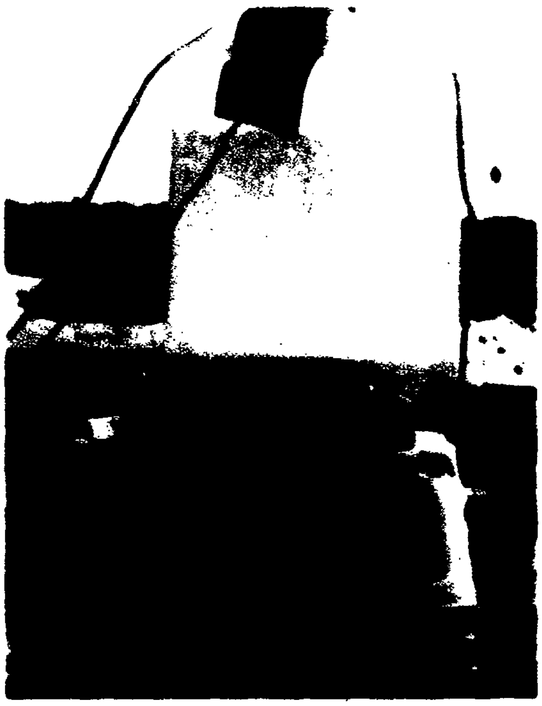

(b) RDX slurry 8-inch container elevated over steel plate with booster of 100 grams of C4 and J2 blasting cap in place.

Figure 4. Typical setups of explosive charges.

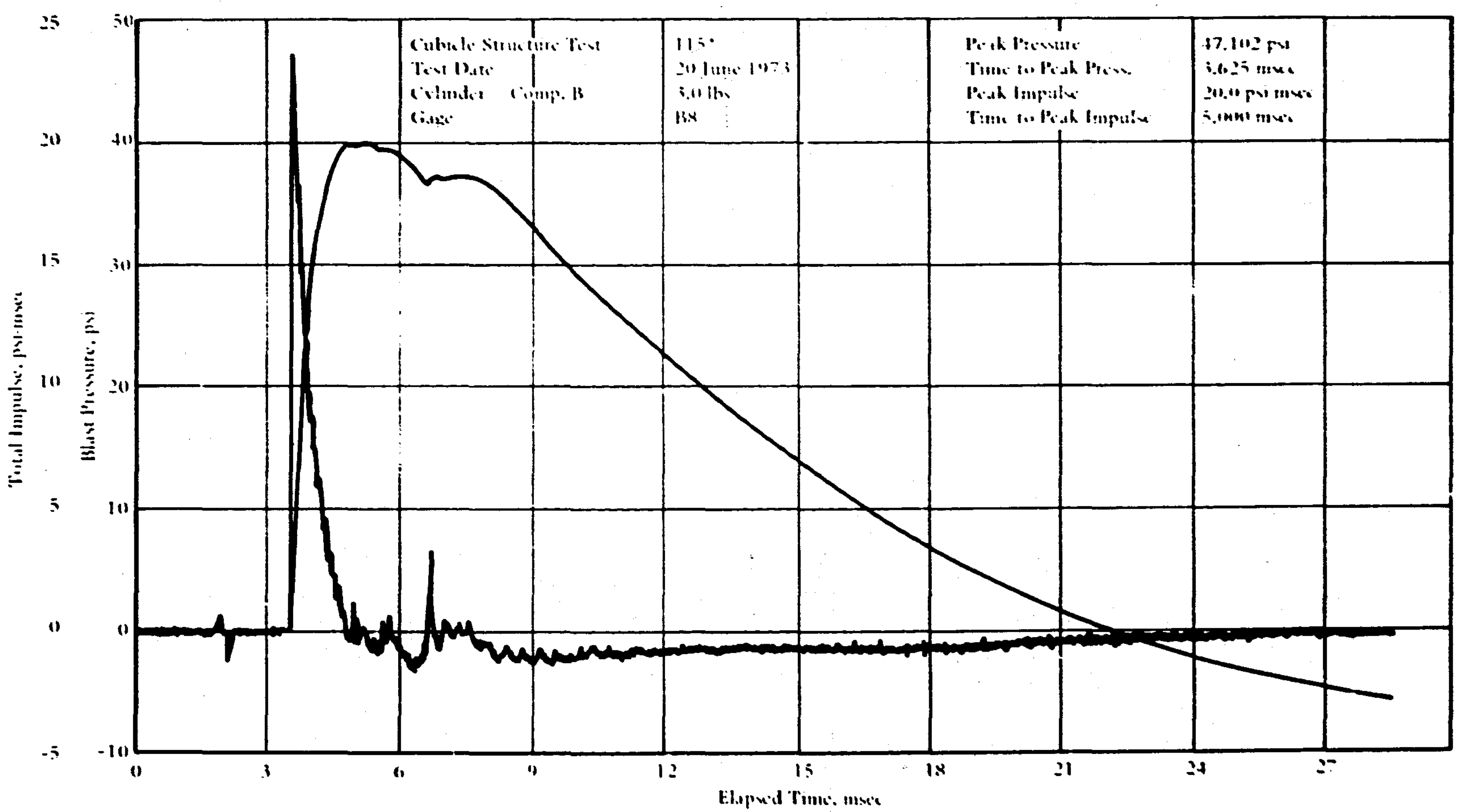

Figure 5. Typical computer plot of digitized pressure-time data.

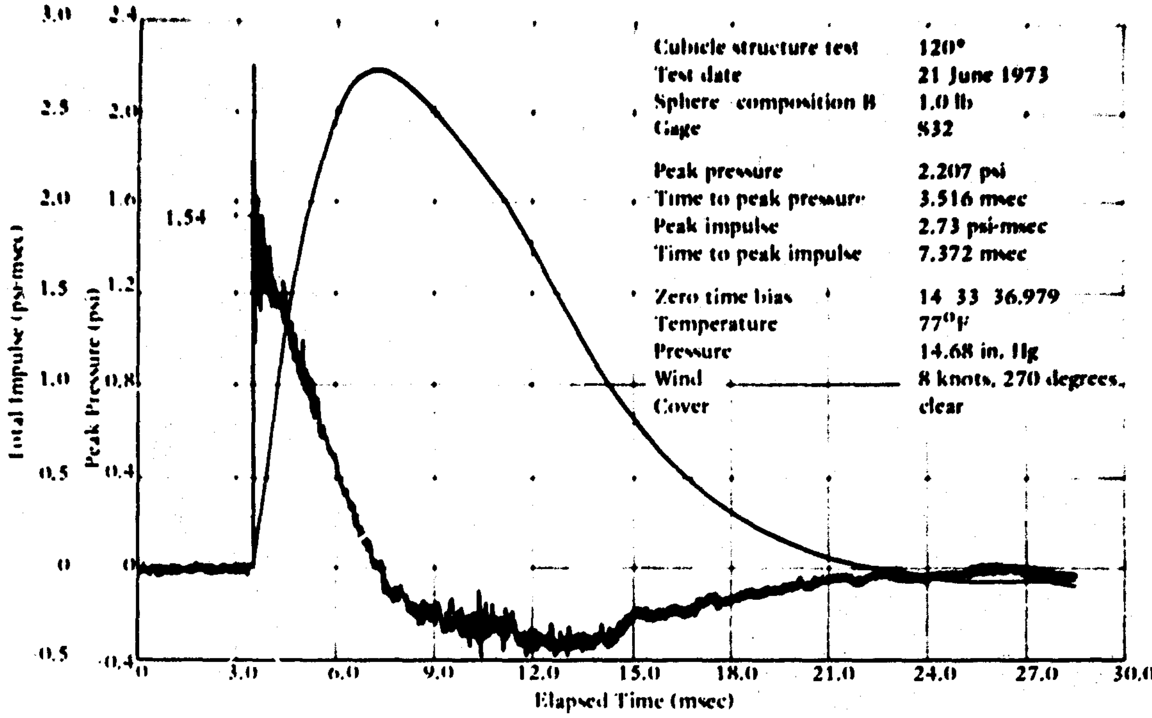

(a) Pressure and impulse versus time.

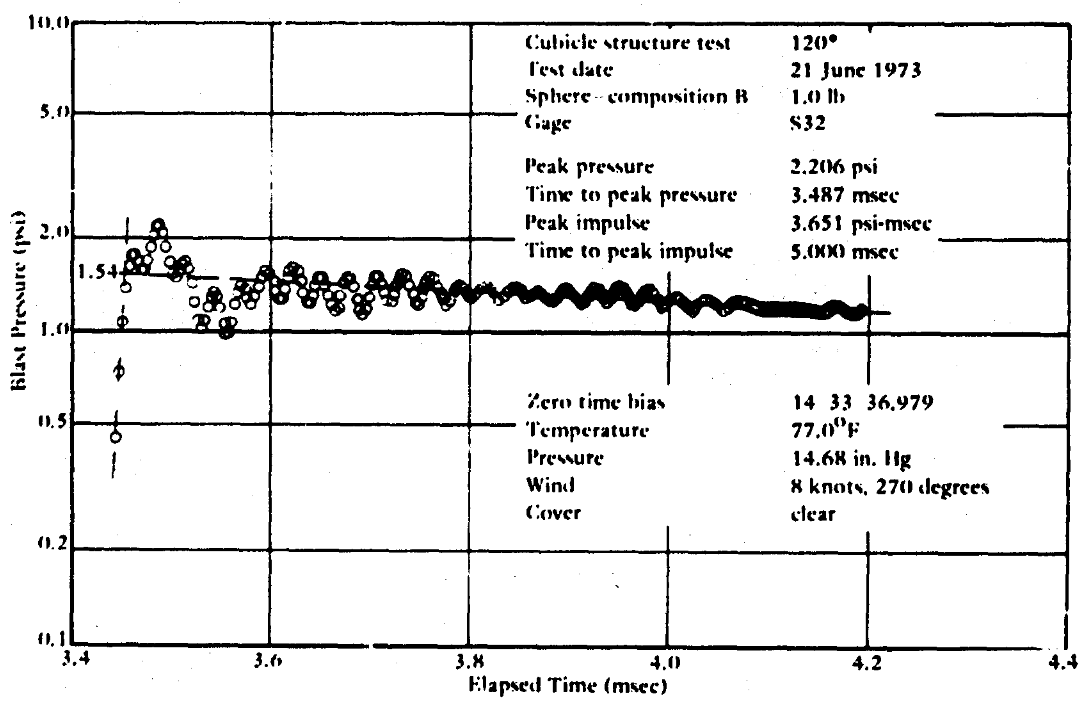

(b) Log pressure versus time.

Figure 6. Computer plots from ''ringing'' pressure transducer, using ''ringing'' gage S32 in 1-pound spherical burst tests.

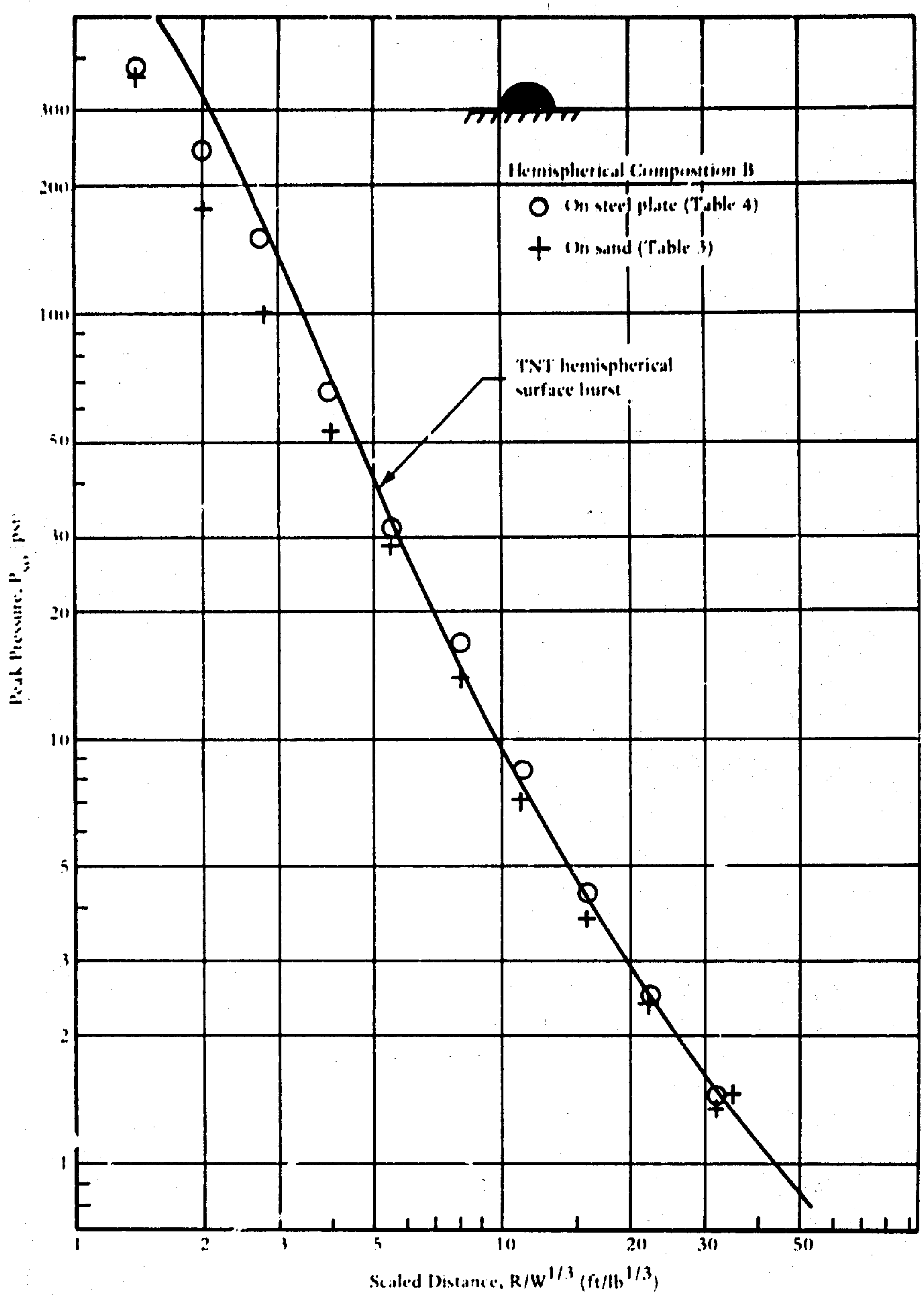

Figure 7. Peak pressure from hemispherical surface burst on sand and on steel plate.

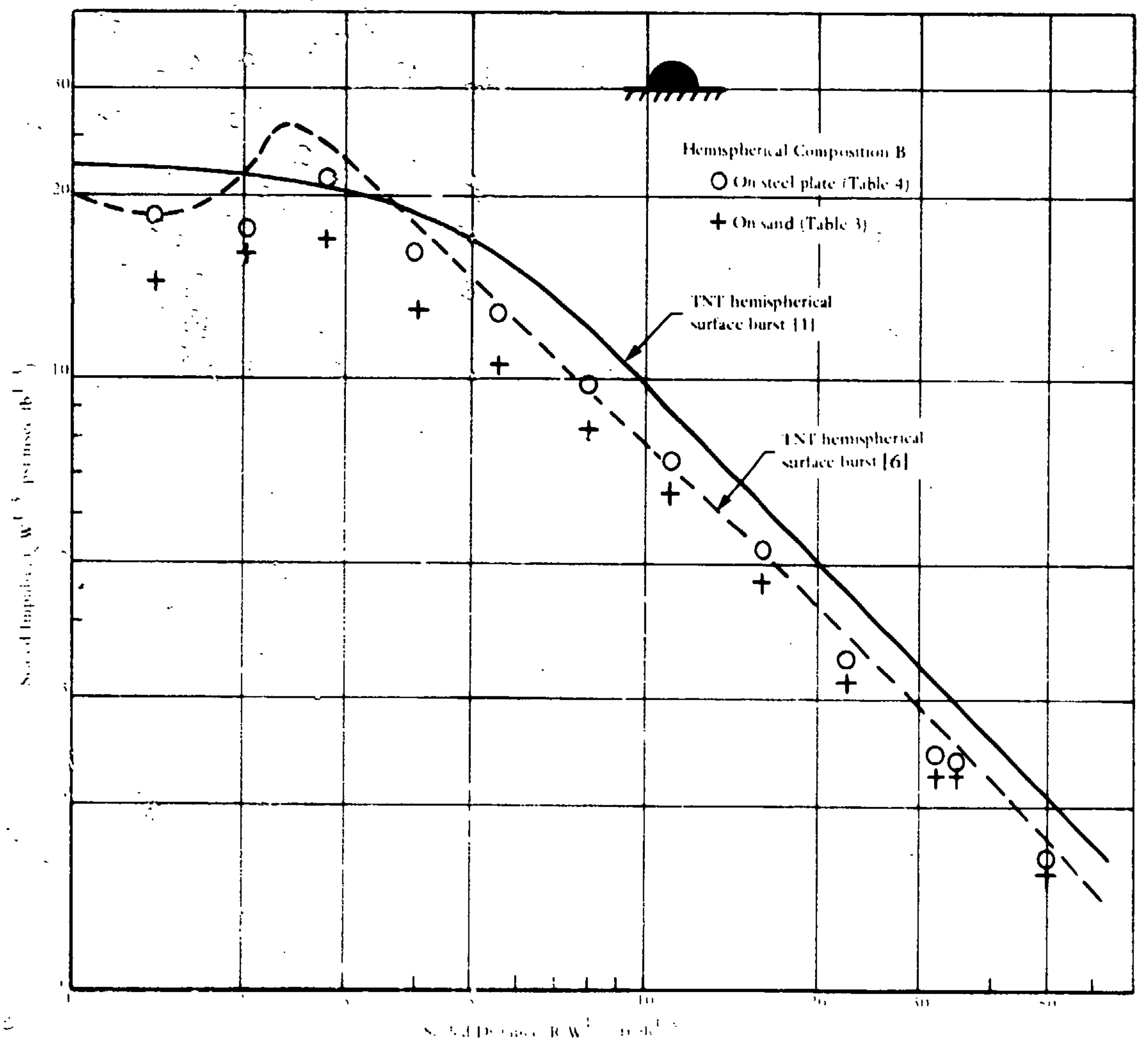

Figure 8. Scaled impulse from hemispherical composition B surface bursts on sand and on steel plate.

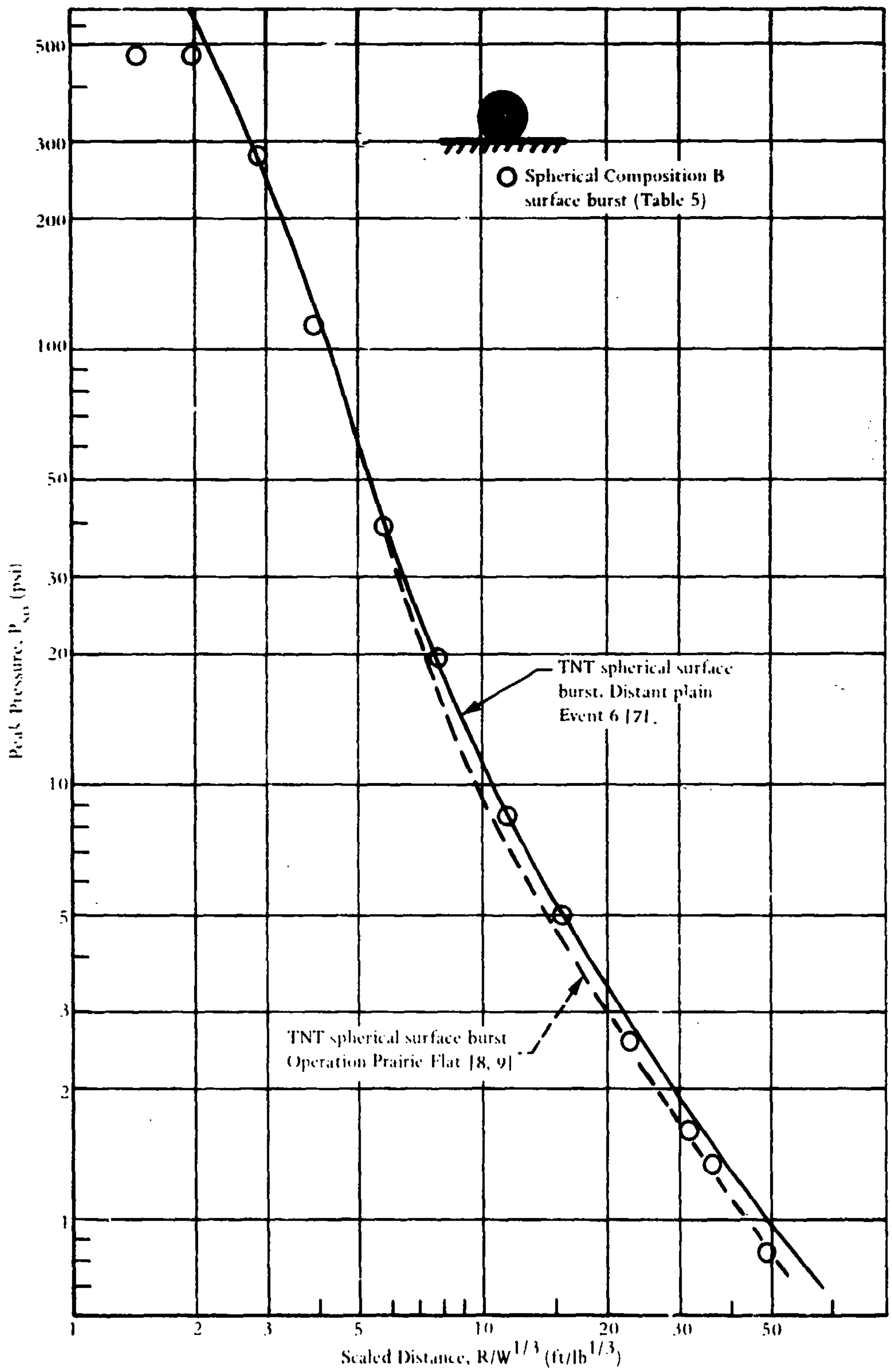

Figure 9. Peak pressure from spherical surface bursts.

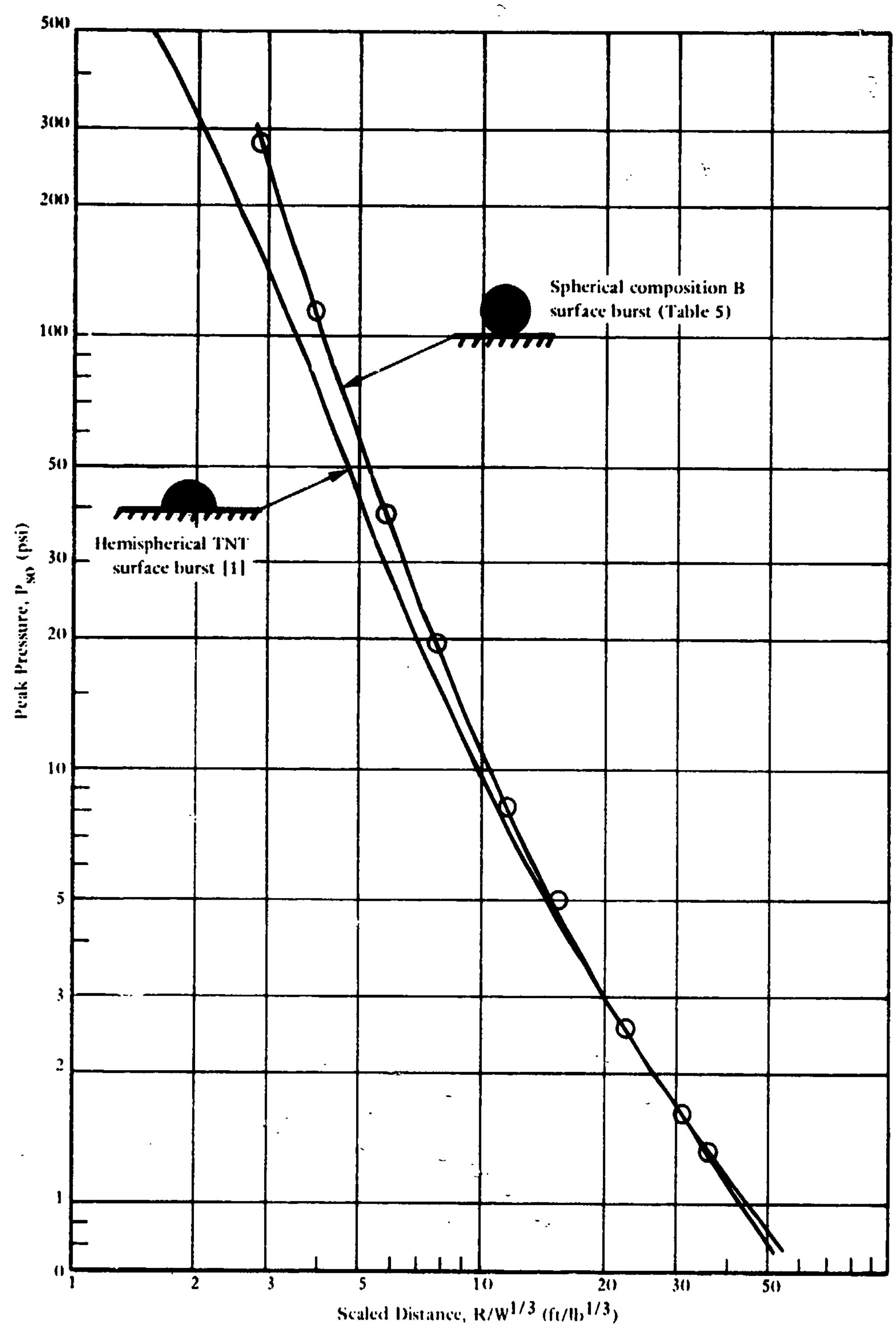

Figure 10. Peak pressure from spherical composition B and hemispherical TNT surface bursts.

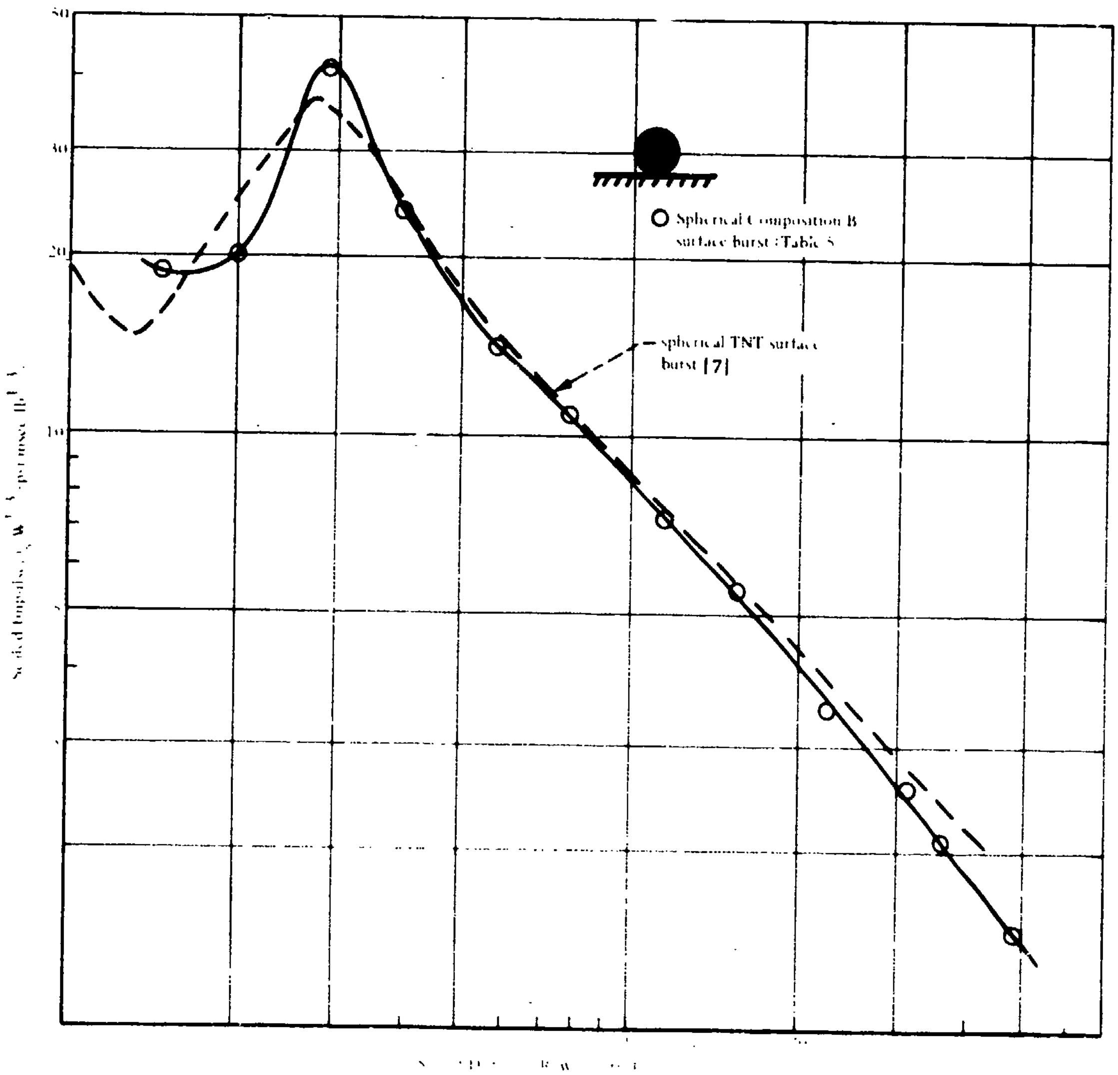

Figure 11. Scaled impulse from spherical surface bursts.

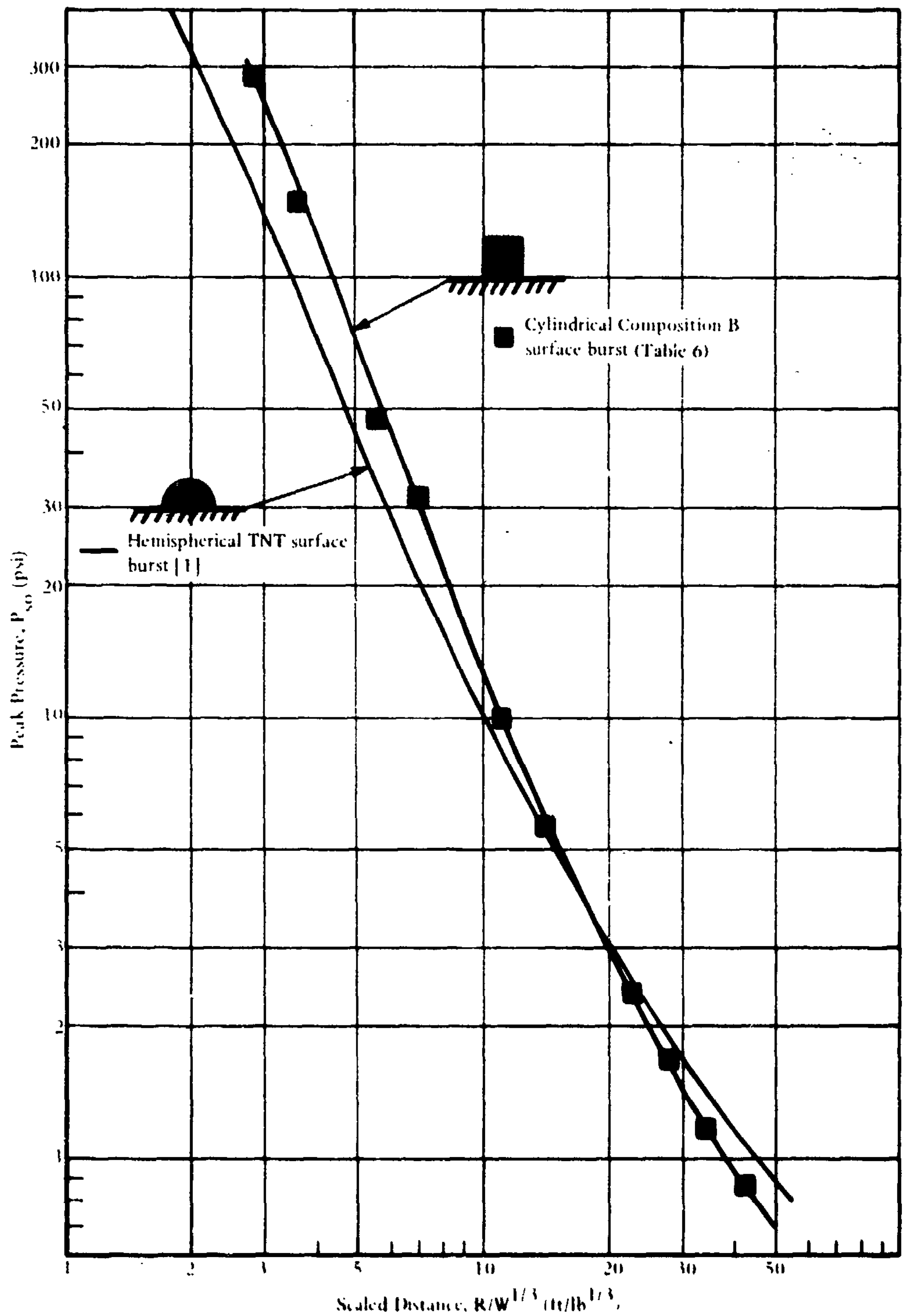

Figure 12. Peak pressure from cylindrical composition B and hemispherical TNT surface bursts.

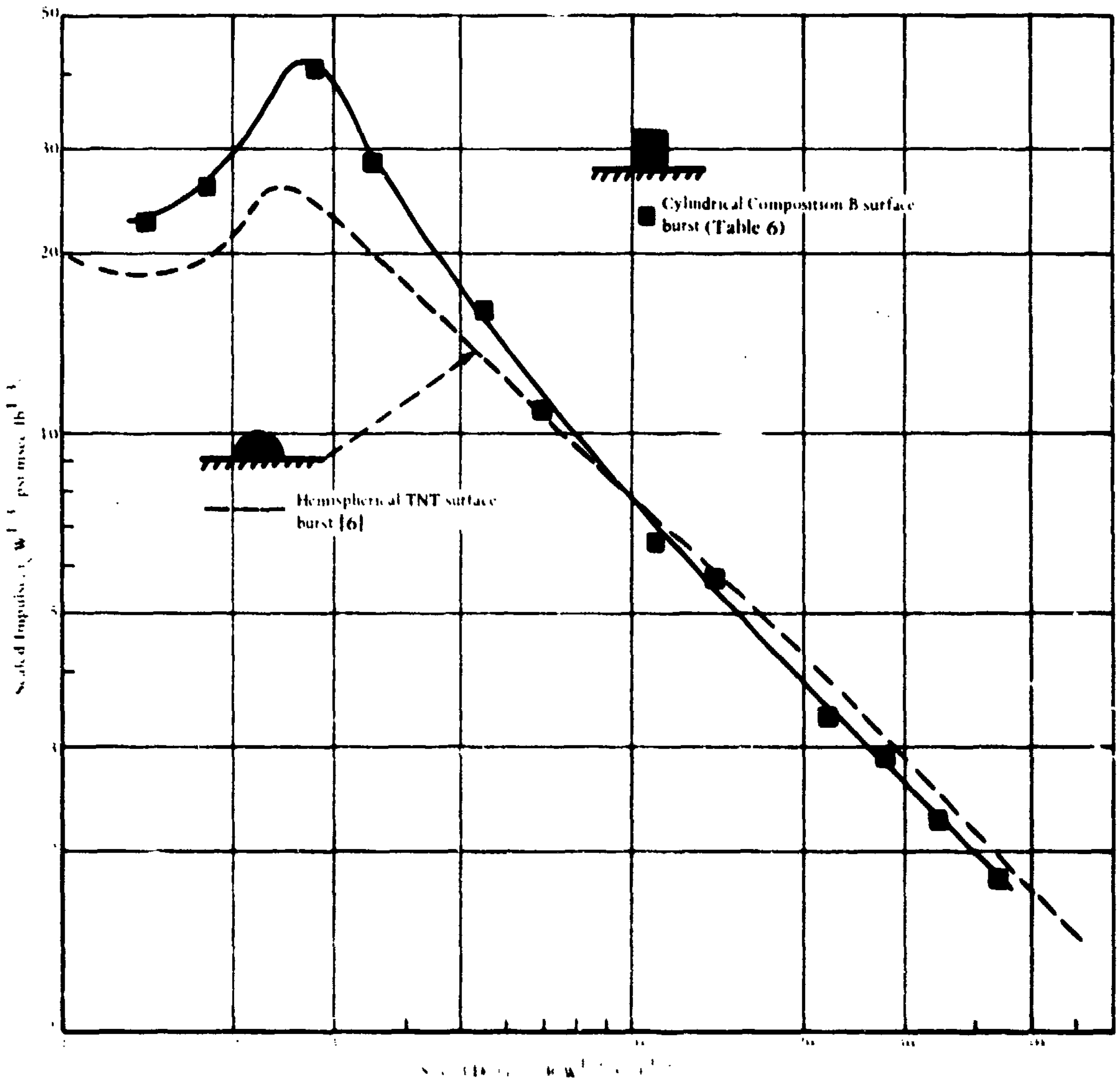

Figure 13. Scaled impulse from cylindrical composition B and hemispherical TNT surface bursts.

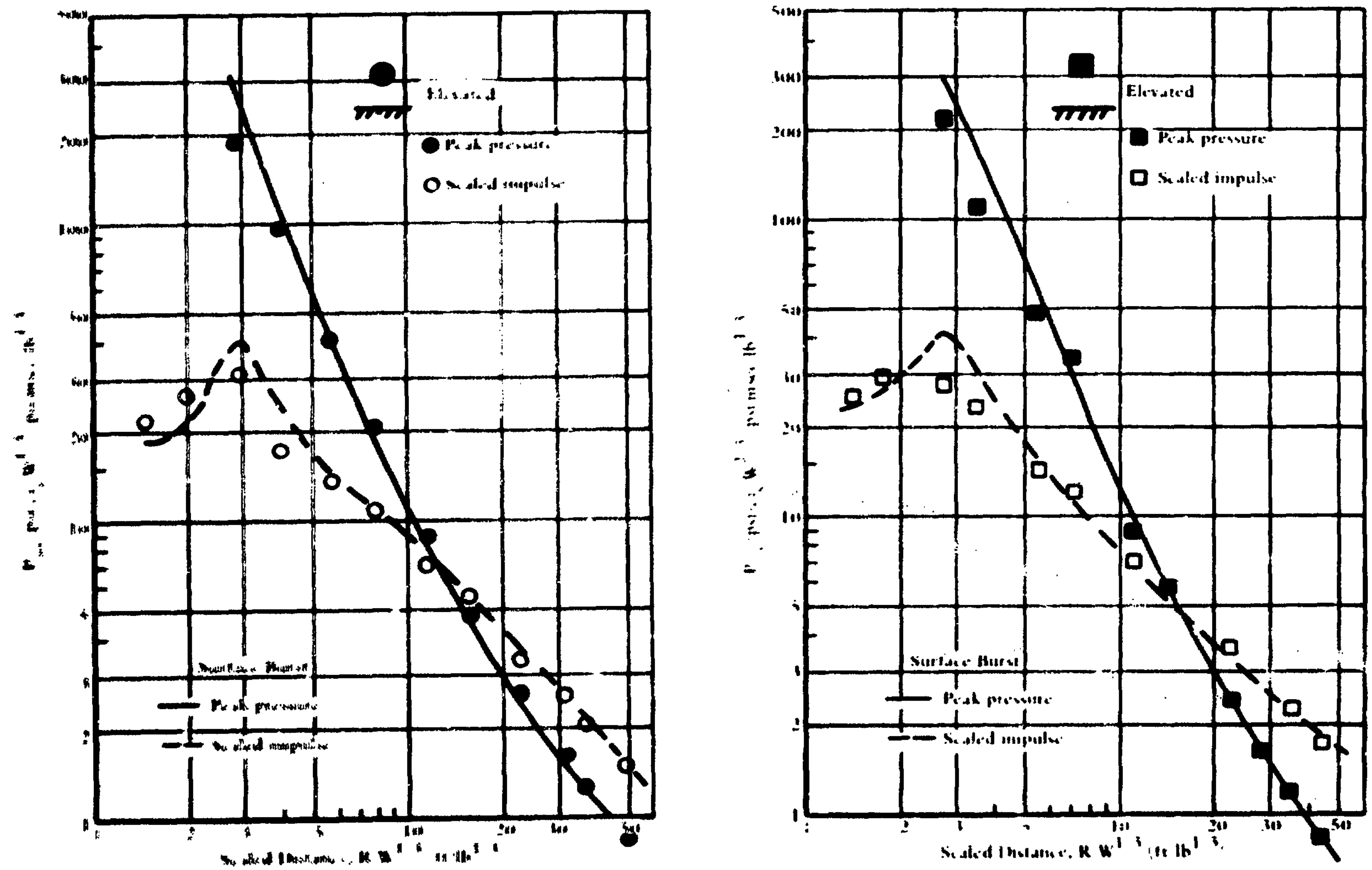

(a) Spherical.

(b) Cylindrical.

Figure 14. Elevated versus surface burst peak pressures and scaled impulses for cylindrical and spherical composition B.

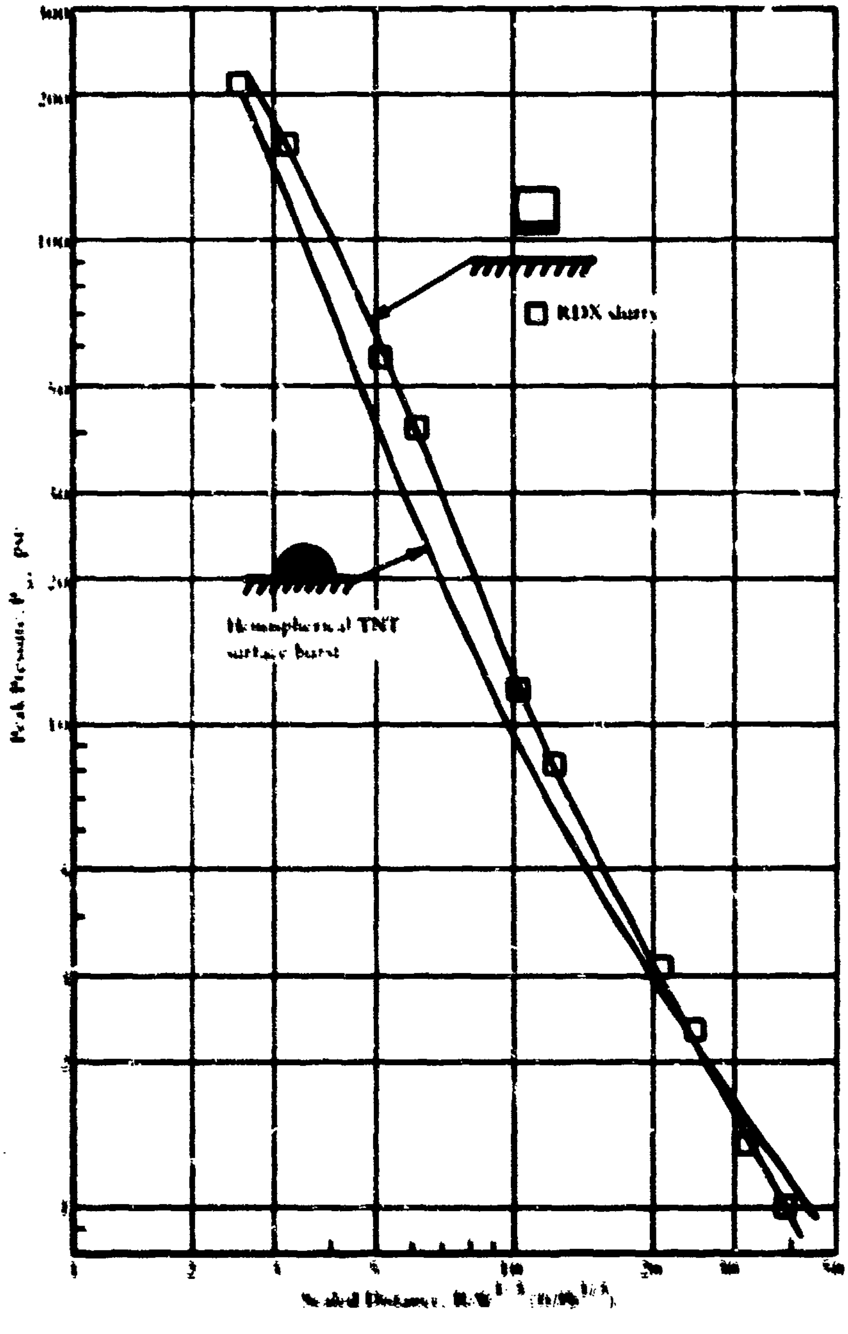

Figure 15. Peak pressure from RDX slurry and hemispherical TNT.

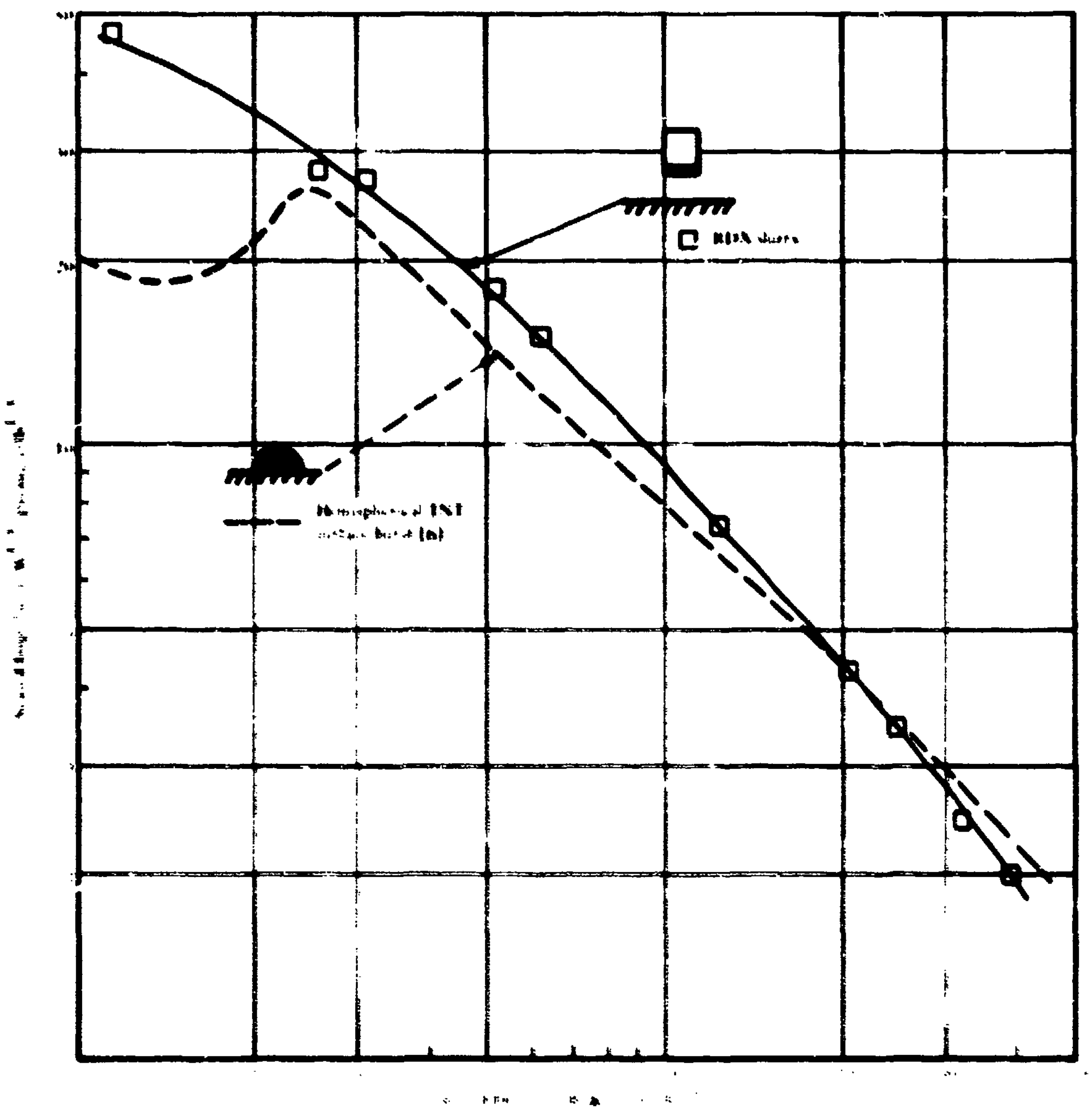

Figure 16. Scaled impulse from RDX slurry and hemispherical TNT.

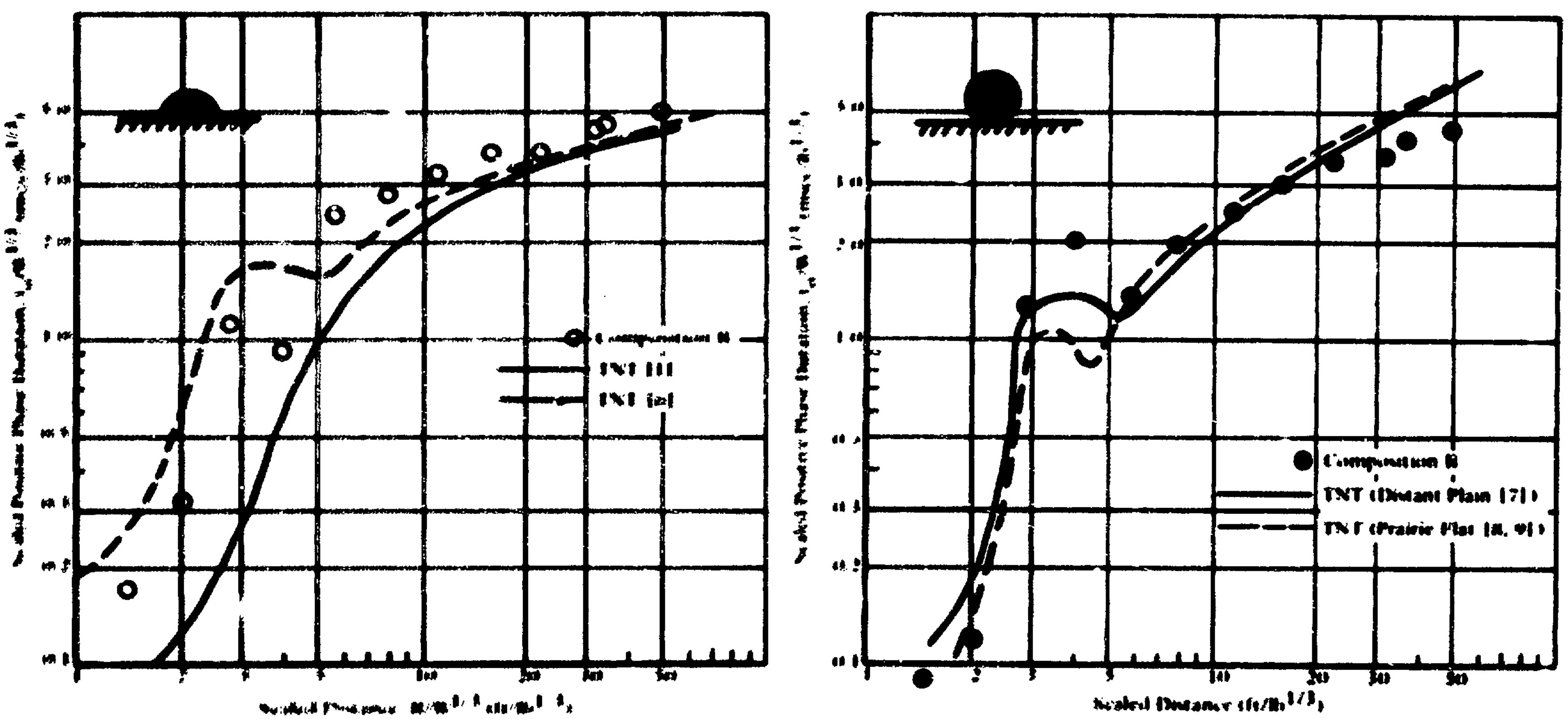

(a) Hemispherical.

(b) Spherical.

Figure 17. Scaled positive phase durations of hemispherical and spherical charges.

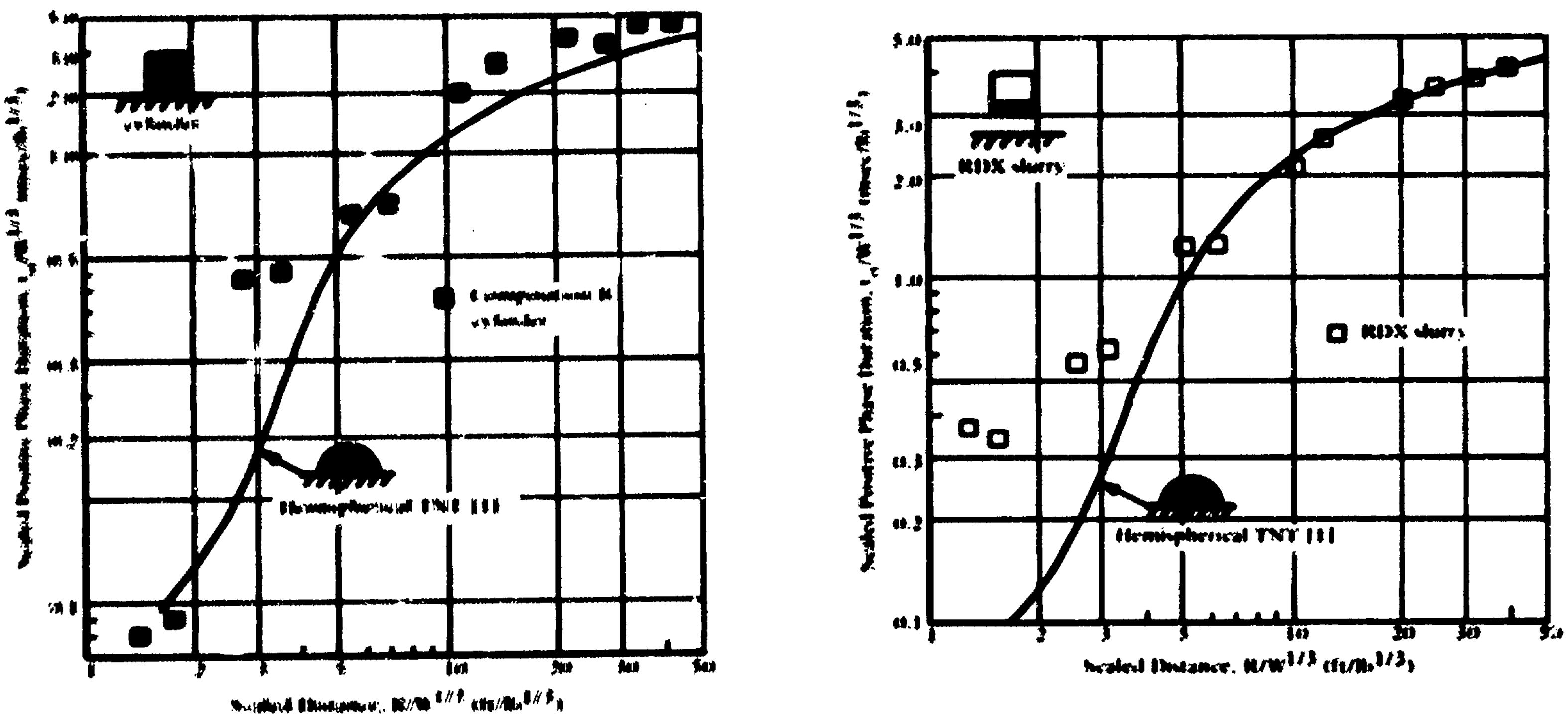

(a) Composition B cylinder and hemispherical TNT.

(b) RDX slurry and hemispherical TNT.

Figure 18. Scaled positive phase durations of composition B cylinders and RDX slurry compared to TNT hemispheres.

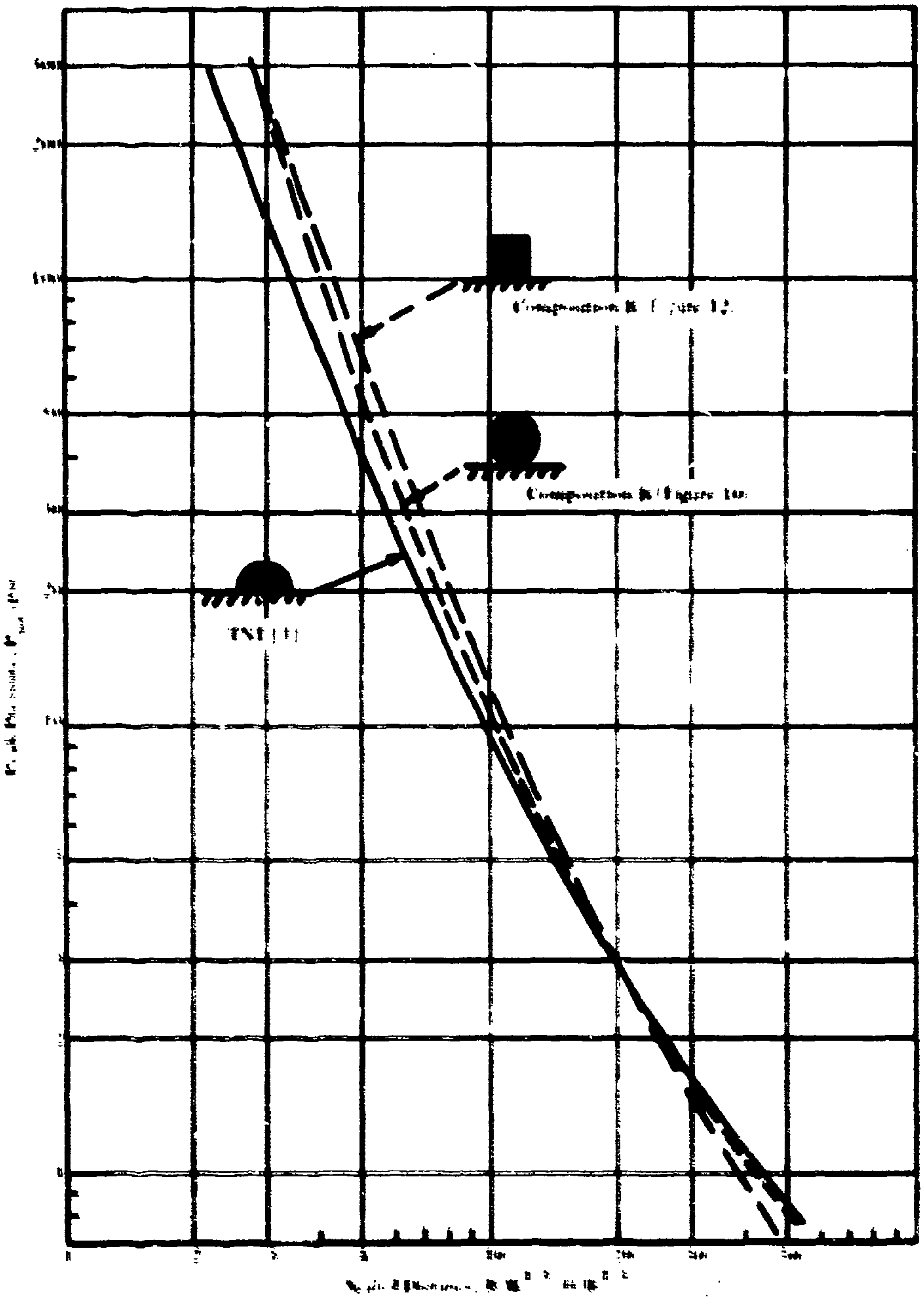

Figure 19. Peak pressure versus scaled distance for spherical, hemispherical, and cylindrical surface bursts.

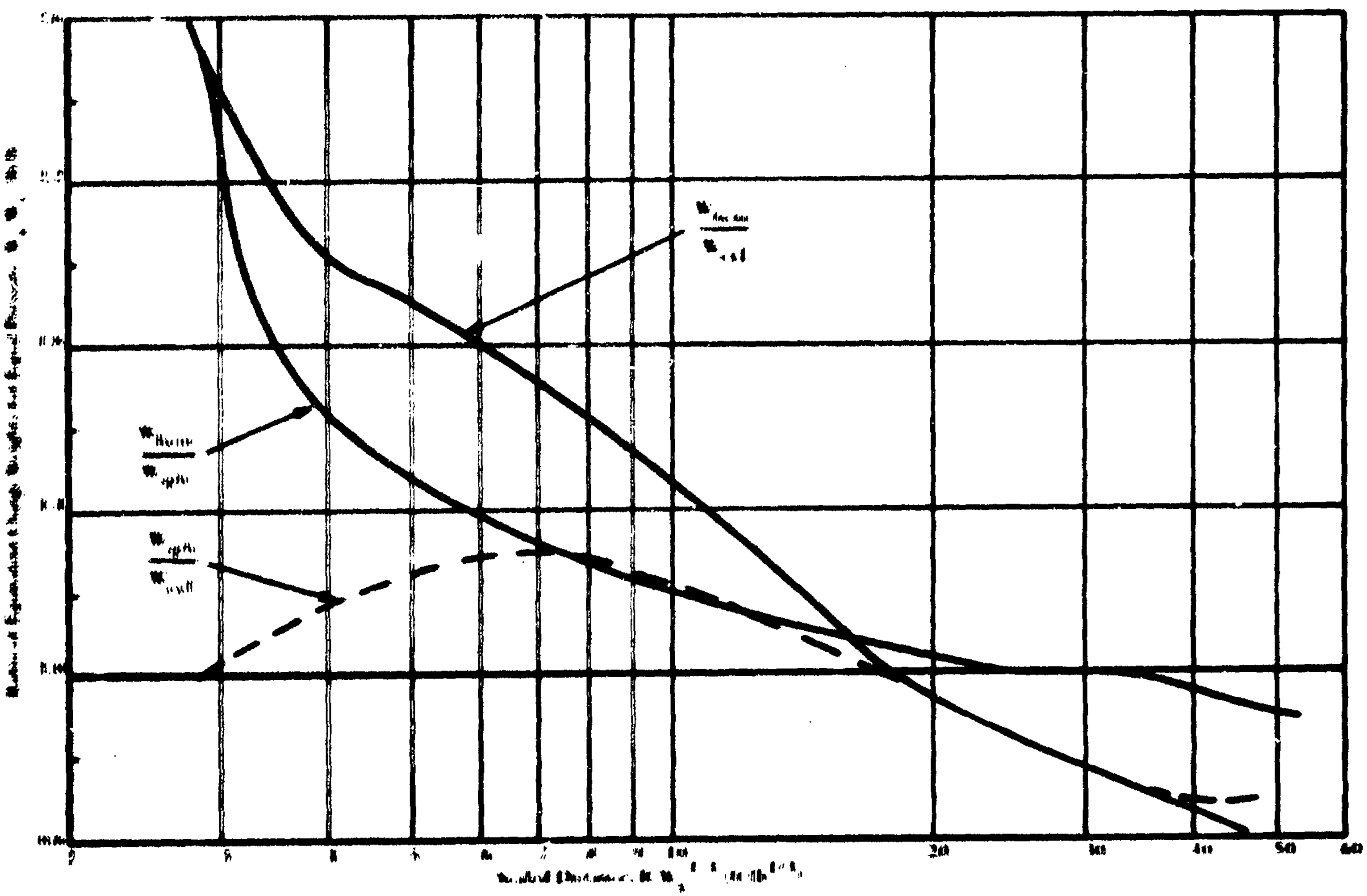

Figure 20. Equivalent weight ratios for equal peak pressures from charges of different shape at the same ground range (Figure 19).

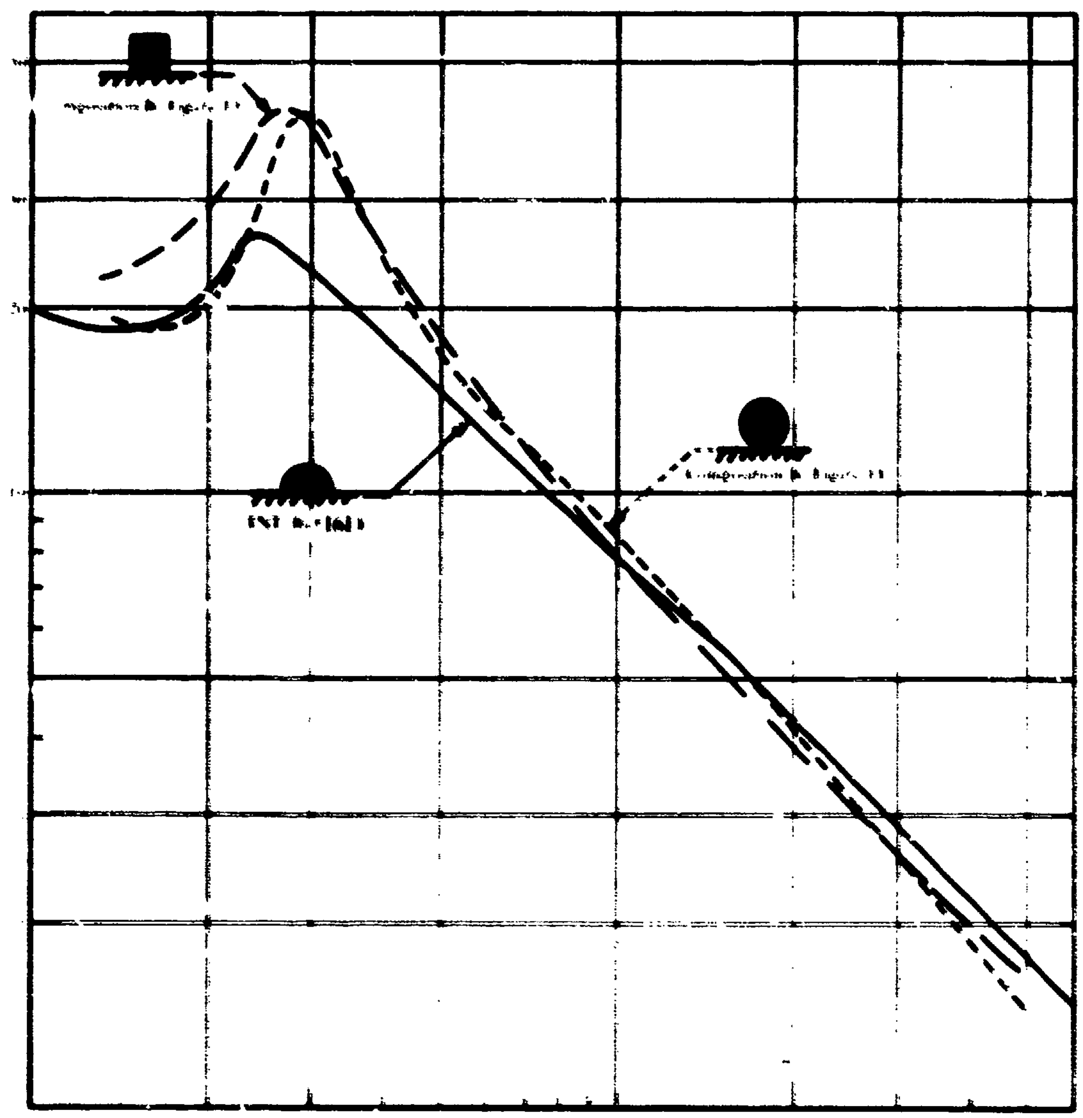

Figure 21. Scaled impulse versus scaled distance for spherical, hemispherical, and cylindrical surface bursts.

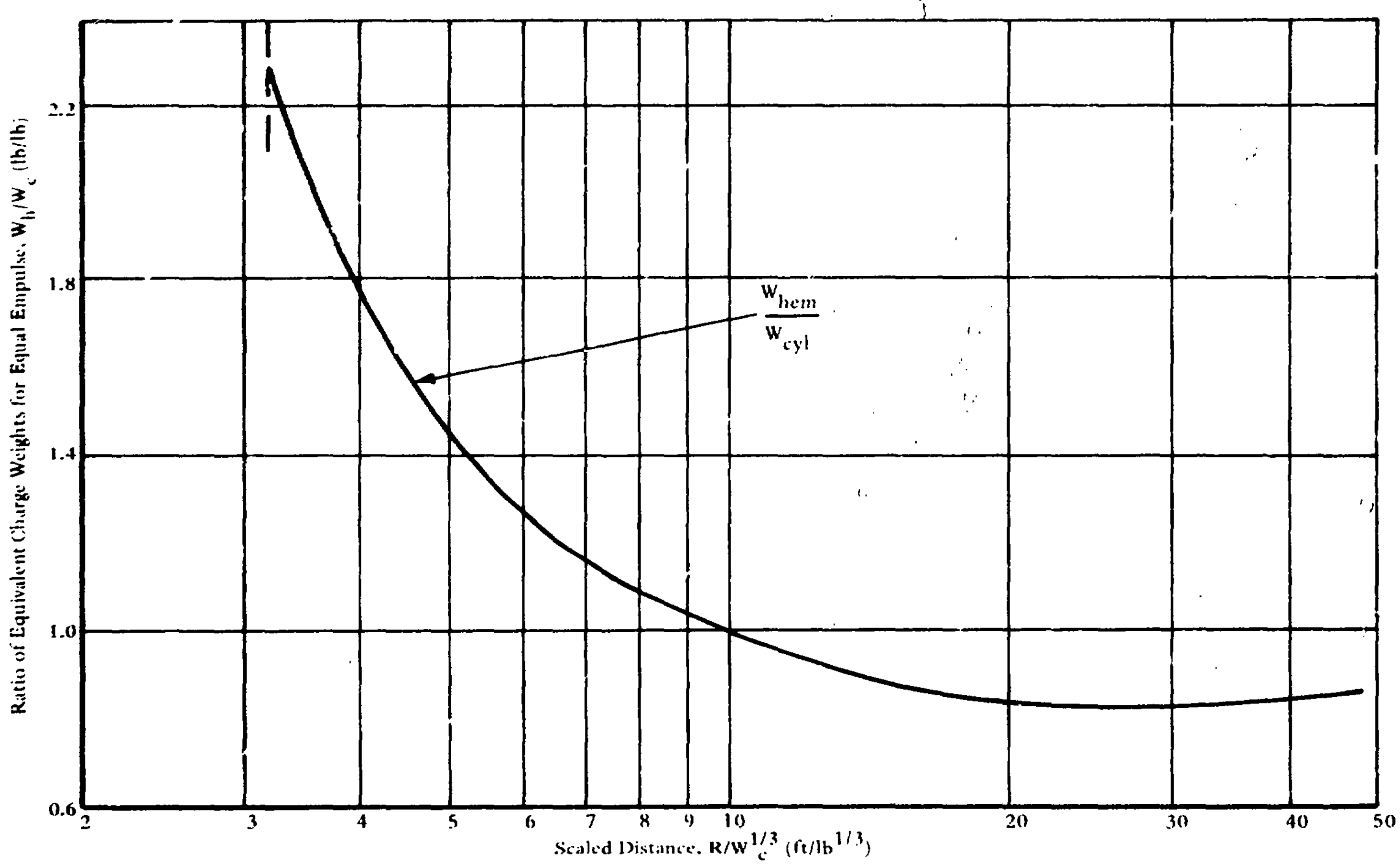

Figure 22. Equivalent weight ratios for equal impulse (psi-msec) from hemispherical and cylindrical surface bursts at the same ground range, R (Figure 21).

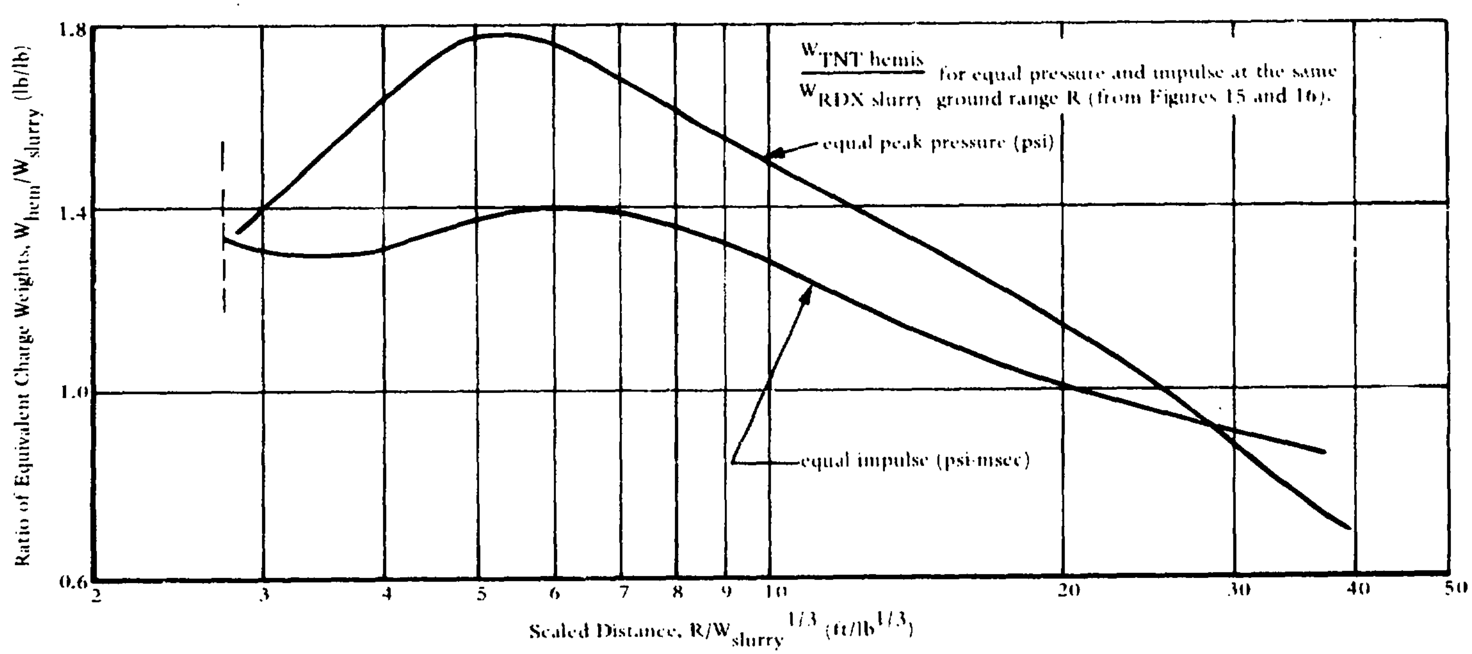

Figure 23. Equivalent weight ratios for equal peak pressure or impulse from RDX slurry and TNT hemispheres.

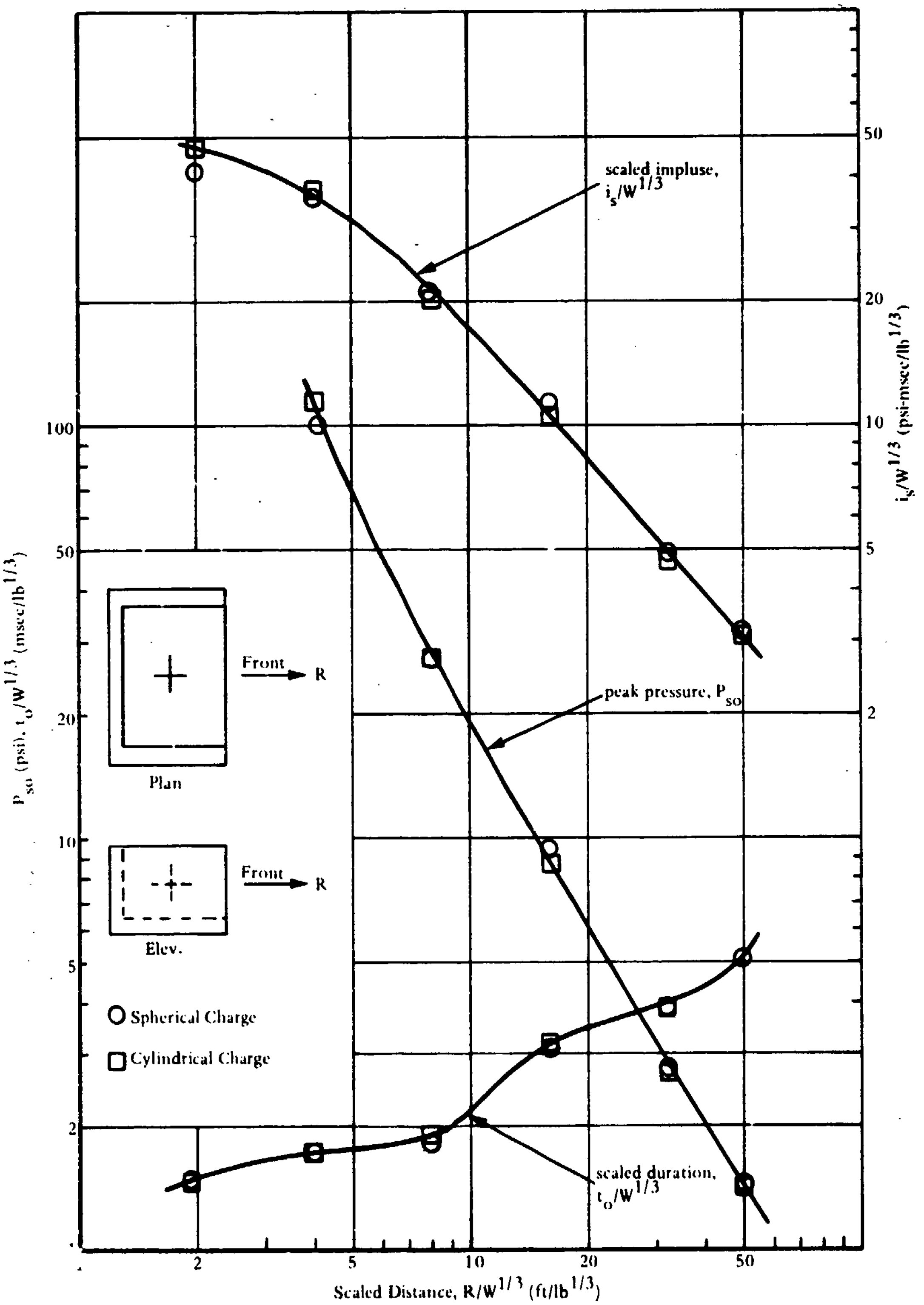

Figure 24. Blast environment parameters out the open wall of cubicle for spherical and cylindrical charges (W = 1.0 pound).

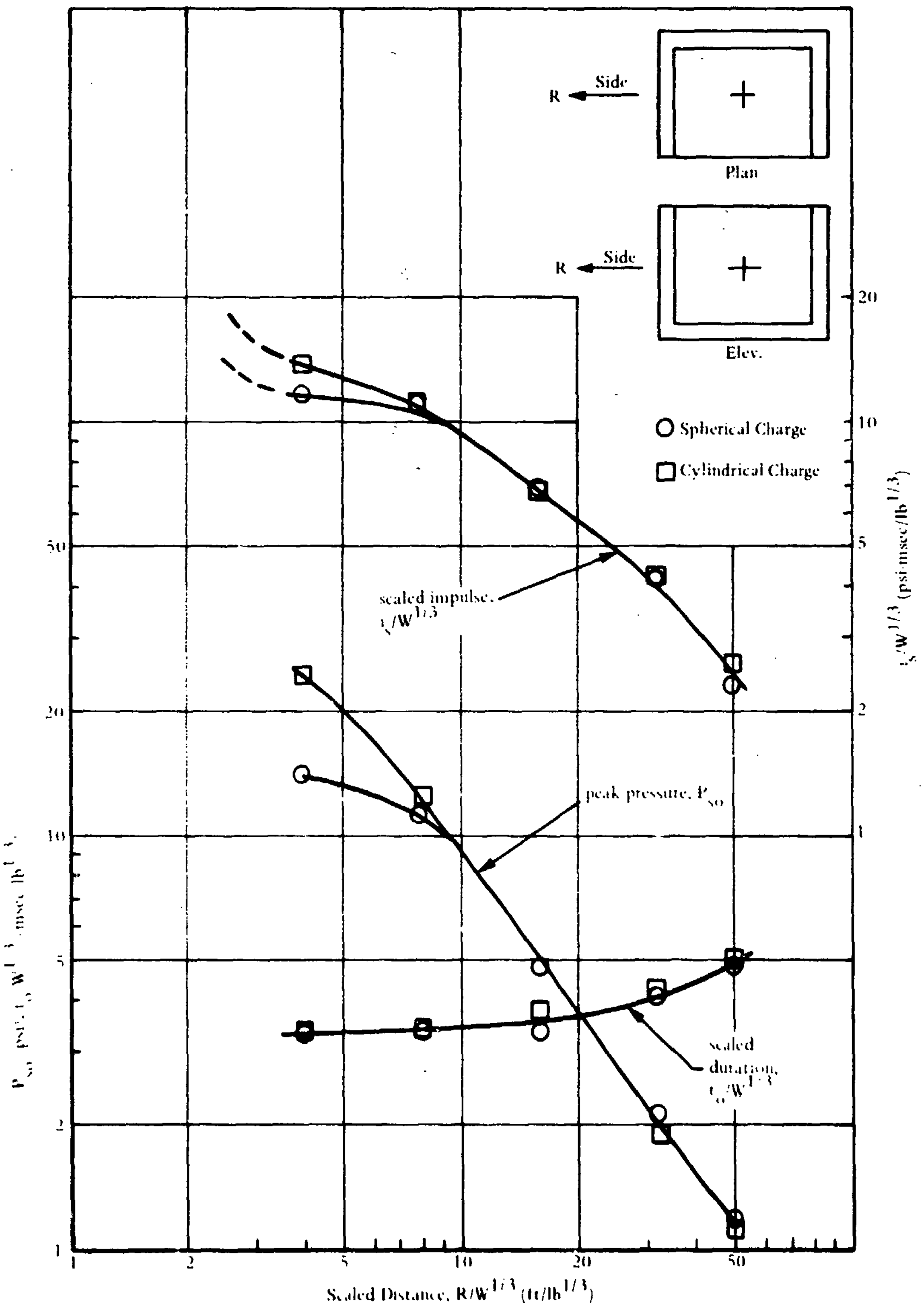

Figure 25. Blast environment parameters behind sidewall of cubicle for spherical and cylindrical charges (W = 1.0 pound).

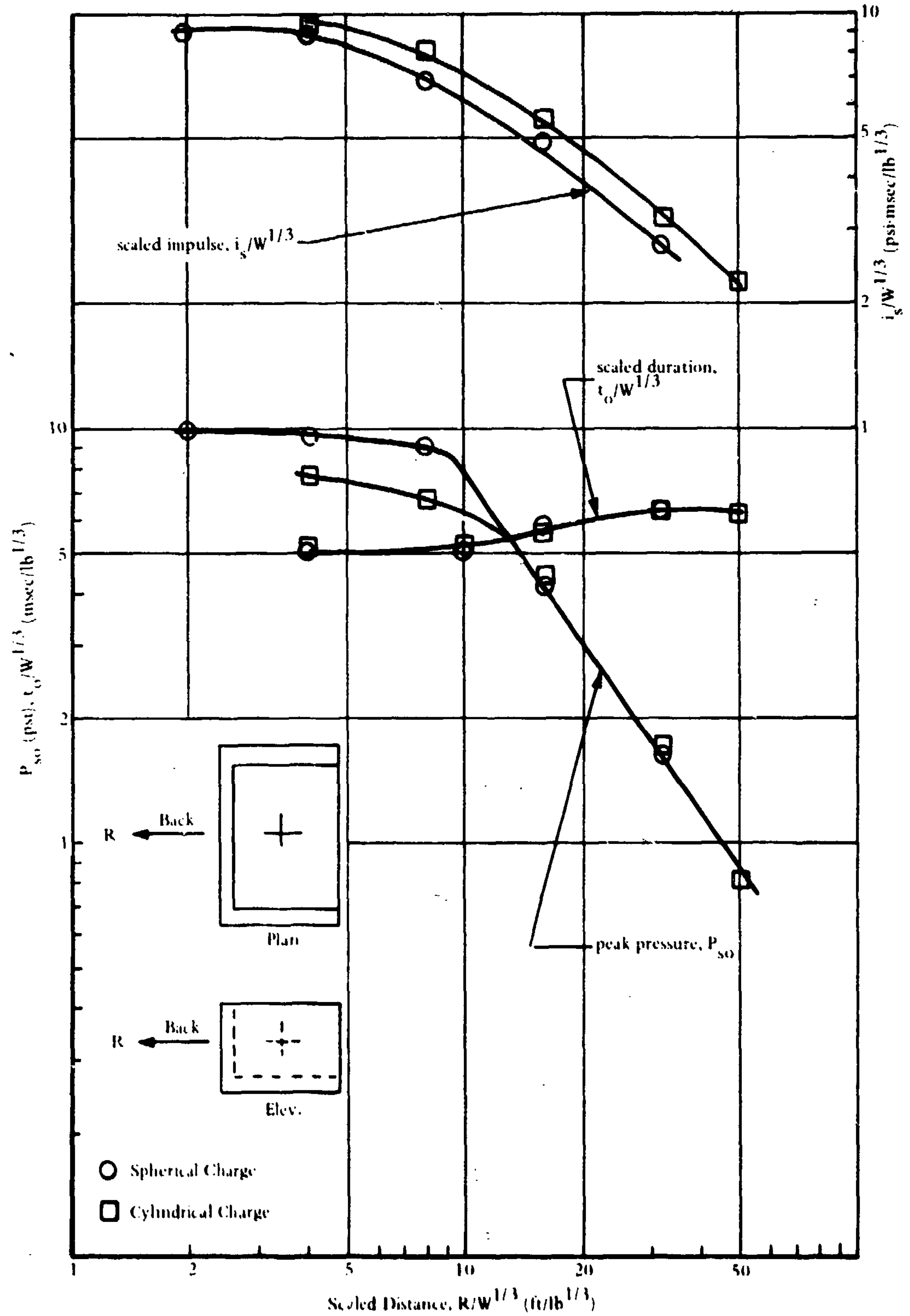

Figure 26. Blast environment parameters behind backwall of cubicle for spherical and cylindrical charges (W = 1.0 pound).

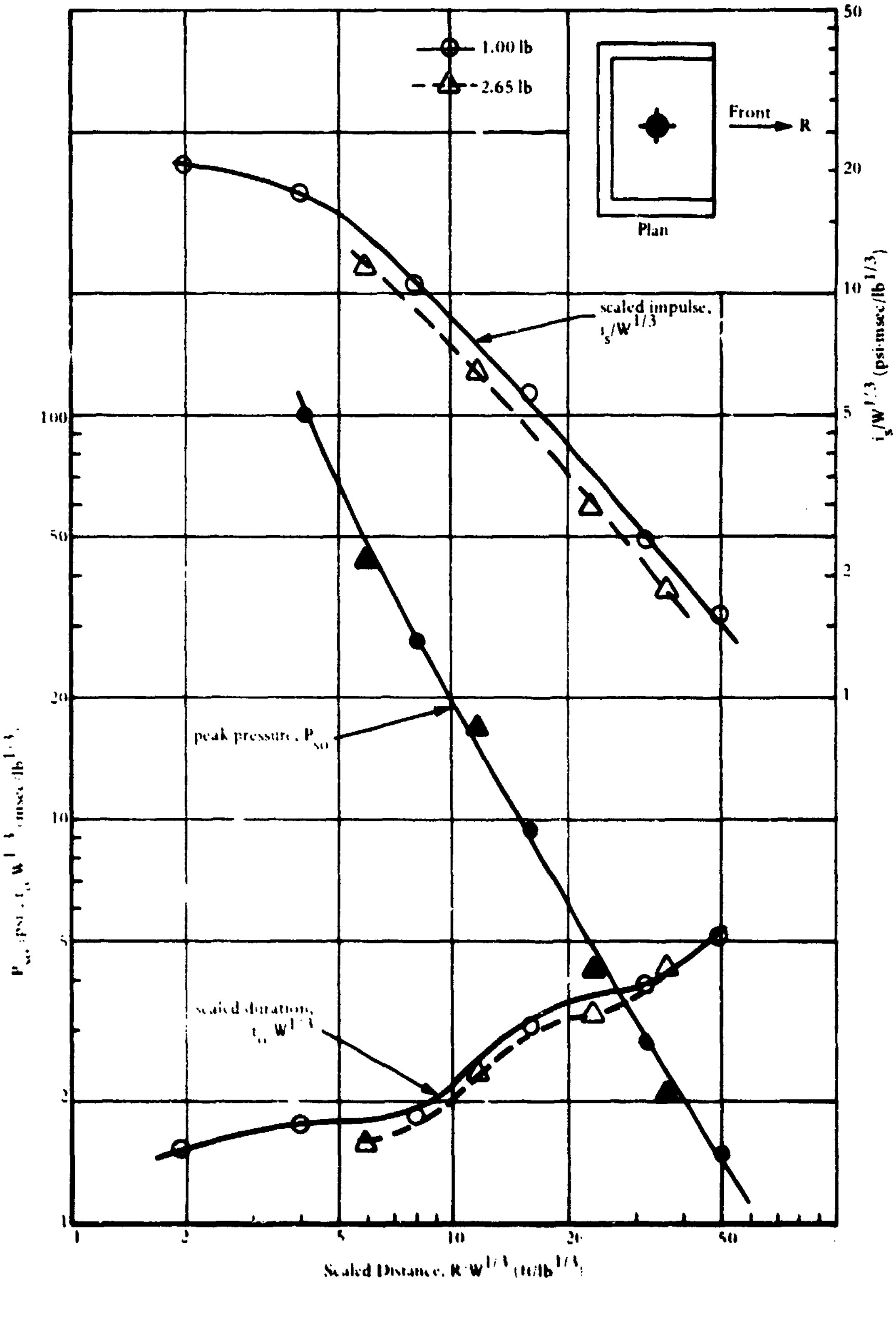

Figure 27. Blast environment parameters out open wall of cubicle for 1.00-and 2.65-pound spherical charges.

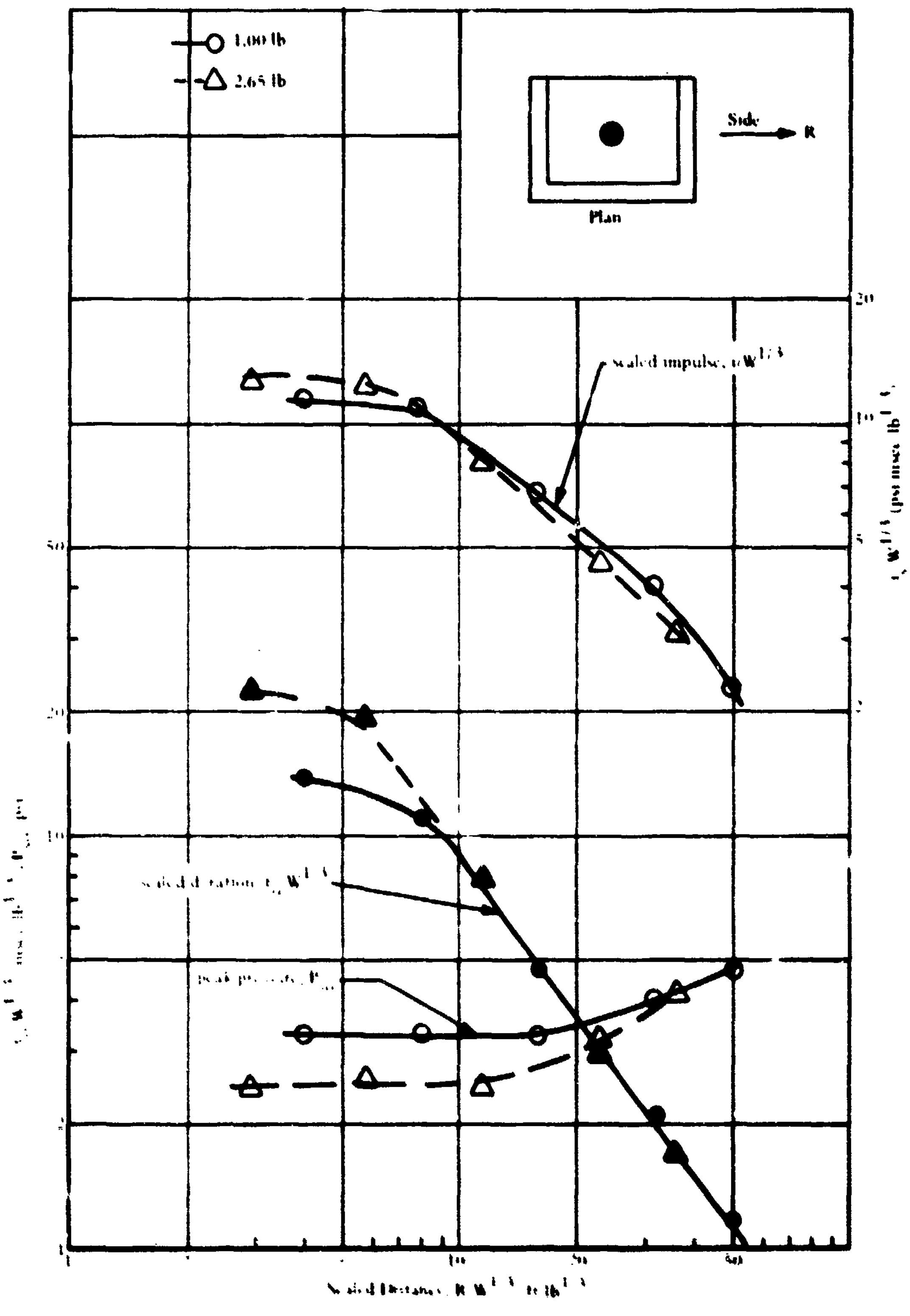

Figure 28. Blast environment parameters behind backwall of cubicle for 1.00- and 2.65-pound spherical charges.

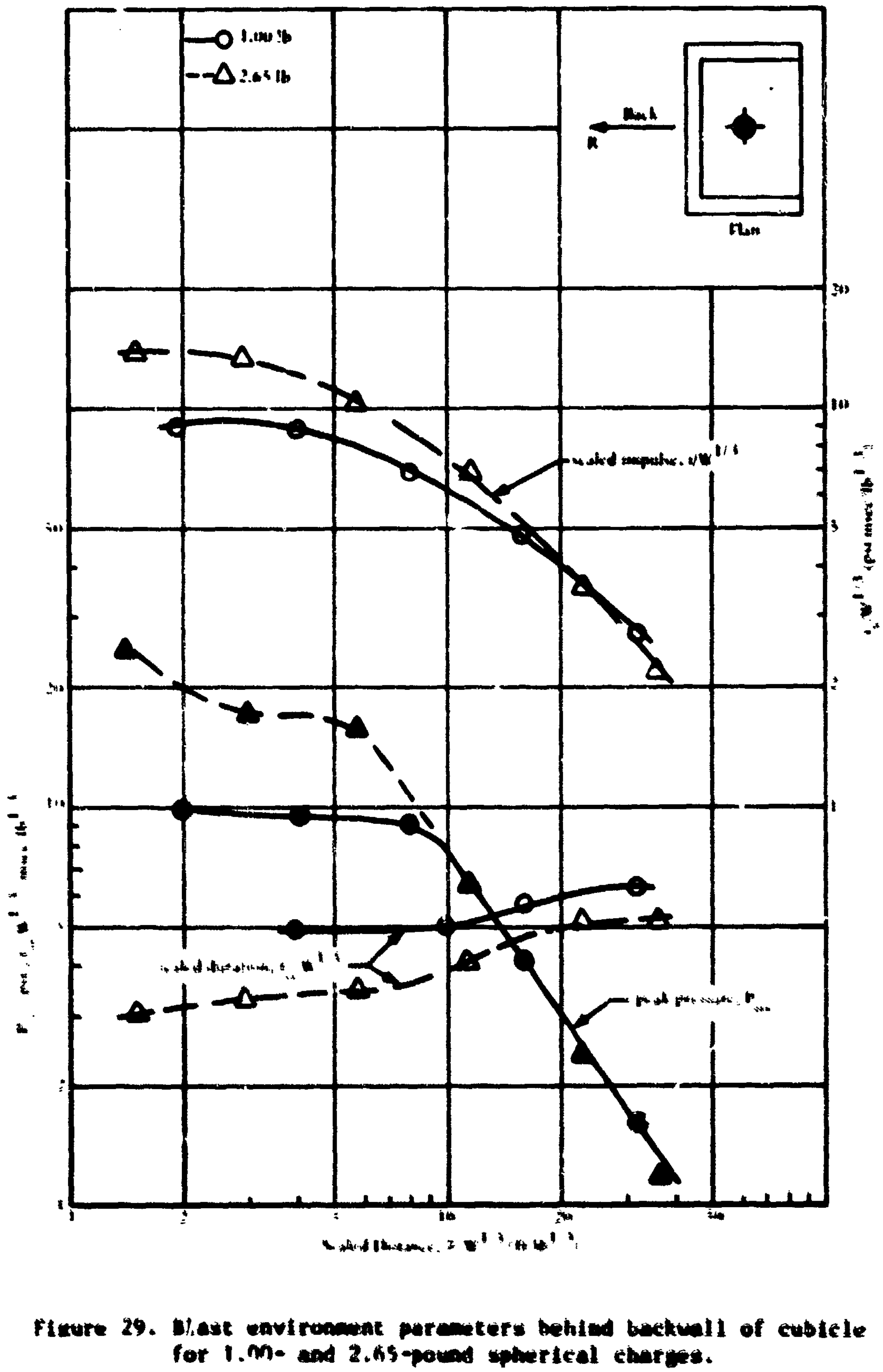

Figure 29. Blast environment parameters behind backwall of cubicle for 1.00- and 2.65-pound spherical charges.

REFERENCES

1. Departments of the Army, Navy and Air Force. TM5-1300/NAVFAC P-397/AFM 88-22: Structures to resist the effects of accidental explosions, Washington, DC, Jun 1969.

2. Civil Engineering Laboratory. Technical Report R- : Blast environment from fully and partially vented explosions in cubicles, by W. A. Keenan and J. E. Tancreto. Port Hueneme, CA (to be published).

3. Naval Ordnance Laboratory. NAVORD Report 2890: Air blast resulting from the detonation of small TNT charges, by E. M. Fisher and J. F. Pittman. White Oak, MD, Jul 1953.

4. Ballistics Research Laboratory. Memorandum Report No. 1691: A procedure for reading and smoothing pressure-time data from H. E. and nuclear explosions, by N. H. Ethridge. Aberdeen Proving Ground, MD, Sep 1965.

5.________. Report No. 466: The dependence of blast on ambient pressure and temperature, by R. G. Sachs. Aberdeen, Proving Ground, MD, May 1944.

6.________. Report No. 1344: Air blast parameters versus distance for hemispherical TNT surface bursts, by C. N. Kingery. Aberdeen Proving Ground, MD, Sep 1966.

7.________. Memorandum Report No. 1955: Air blast measurements from the detonation of large spherical TNT charges resting on the surface (Operation Distant Plain, Events 6A, 6), by Ralph E. Reister, Noel H. Ethridge, and Louis Giglio-Tos. Aberdeen Proving Ground, MD, Jan 1969.

8. Defense Atomic Support Agency. POR-2100: Prairie Flat event, fundamental blast studies, by L. Giglio-Tos and B. A. Pettot. Washington, DC, Mar 1971.

9. General Electric Company. Operation Prairie Flat Symposium Report: Volume 1, Part 1, by DASA Information and Analysis Center. Santa Barbara, CA, Jan 1970.

10.________. Report No. 681: Comparison of the blast from explosive charges of different shapes, by C. L. Adams, J. N. Sarmousakis, and J. Sperrazza. Aberdeen Proving Ground, MD, Jan 1949.

11. Denver Research Institute. Characteristics of blast waves obtained from cylindrical high explosive charges, by John Wisotski and William H. Snyer. Denver, CO, Nov 1965.

12. Ballistics Research Laboratories. Interim Memorandum Report No. 42: Air blast from one pound cylindrical charges positioned vertically on the ground, by R. E. Reisler and D. P. LeFevre. Aberdeen Proving Ground, MD, Apr 1972.

DISTRIBUTION LIST

SNDL Code	No. of Activities	Total Copies	
	1	12	Defense Documentation Center
	1	10	Picatinny Arsenal
FKA1C	1	3	Naval Facilities Engineering Command
FKN1	6	6	NAVFAC Engineering Field Divisions
FKN5	9	9	Public Works Centers
FA25	1	1	Public Works Center
-	6	6	RDT&E Liaison Officers at NAVFAC Engineering Field Divisions and Construction Battalion Centers
	292	294	CEL Special Distribution List No. 15 for persons and activities interested in reports on Structural Mechanics